MARMARA UNIVERSITY

FACULTY OF ENGINEERING

Dynamic Analysis and Vibration Simulation of a Steam Turbine

Hüseyin Nüsret Yıldırım, Ayhan Bakır

GRADUATION PROJECT REPORT

Department of Mechanical Engineering

Supervisor

Assoc. Prof. İBRAHİM SİNA KUSEYRİ

MARMARA UNIVERSITY

FACULTY OF ENGINEERING

Rotor Design, Dynamic Analysis and

Vibration Simulation of a Steam Turbine

by

Hüseyin Nüsret Yıldırım, Ayhan Bakır

Jun 07, 2024, Istanbul

SUBMITTED TO THE DEPARTMENT OF MECHANICAL ENGINEERING IN PARTIAL FULFILLMENT OF THE REQUIREMENTS FOR THE DEGREE

OF

BACHELOR OF SCIENCE

AT

MARMARA UNIVERSITY

Signature of Author(s) .....Hüseyin Nüsret Yıldırım, Ayhan Bakır

Department of Mechanical Engineering

Certified By .....Assoc. Prof. İBRAHİM SİNA KUSEYRİ

Project Supervisor, Department of Mechanical Engineering

Accepted By..... Prof. Dr. Bülent EKİCİ

Head of the Department of Mechanical Engineering

ACKNOWLEDGEMENT

First of all, I would like to thank my supervisor Assoc. Prof. İBRAHİM SİNA KUSEYRİ, for the valuable guidance and advice on preparing this thesis and giving me moral and material support.

JUN, 2024

Hüseyin Nüsret Yıldırım, Ayhan Bakır

CONTENTS

ABSTRACT

Dynamic Analysis and Vibration Simulation of a Steam Turbine

Since the advent of steam turbines, it has been a common experience that vibrations of rotors are the main causes of breakdown. In addition, recently, steam turbines with large capacity have been operated under severer conditions such as high loading and high rotational speed. Therefore, the vibration problem becomes easier to occur on the modern steam turbine. In order to develop the steam turbine with high reliability, it is indispensable to exactly predict the vibration characteristics at the design stage and to prevent harmful vibration. In this project we will use a developed FE code to analyze and simulate the vibration characteristics of a steam turbine.

SYMBOLS

$\boldsymbol{\Omega}$: Angular Speed of the Rotor

$\boldsymbol{\zeta}$: Damping Ratio

$\boldsymbol{\omega_n}$: Natural Frequency

$\boldsymbol{m}$: Mass of the System

$\boldsymbol{c}$: Damping Coefficient

$\boldsymbol{k}$: Elastic Coefficient of the System

$\boldsymbol{\Phi}$: Phase Angle

T : Period

$\boldsymbol{\omega_d}$: Damped Frequency

t : Time

$\boldsymbol{k_T}$: Translational Stiffness

$\boldsymbol{k_C}$: Elastic Couplings between displacements and rotations

$\boldsymbol{k_R}$: Rotational Stiffness

$\boldsymbol{I_d}$: Diametral Moment of Inertia

$\boldsymbol{I_p}$: Polar Moment of Inertia of the Motor

$\boldsymbol{\omega_c}$: Critical Speed Frequency

$\boldsymbol{\omega_R}$: Resonance Speed Frequency

$\boldsymbol{Hz}$: Hertz

$\boldsymbol{x_1, x_2}$: Generalized coordinates

$\dot{x}_1, \dot{x}_2$: Vector of generalized velocities

$\ddot{x}_1, \ddot{x}_2$: Vector of generalized accelerations

$[M]$: $n \times n$ generalized mass or inertia matrix

$[C]$: $n \times n$ generalized damping matrix

$[K]$: $n \times n$ generalized stiffness matrix

$\{\ddot{q}\}$: n-dimensional column vector of generalized accelerations

$\{\dot{q}\}$: n-dimensional column vector of generalized velocities

$\{q\}$: n-dimensional column vector of generalized coordinates

$\{Q\}$: n- dimensional column vector of generalized nonconservative external forces (excluding the damper forces)

X : Mode Shape Vector

l_e : Length of the element

ε : Eccentricity

η : Absolute viscosity of the oil

c : Bearing radial clearance

f_r : Radial force

f_t : Tangential force

S_s : Modified Sommerfeld number or Ocvirk number

S : Sommerfeld number

K_{xx} : Horizontal stiffness

K_{yy} : Vertical damping

C_{xx} : Sommerfeld number

C_{xx} : Sommerfeld number

ε : Eccentricity

u : Displacement of the rotor's center of mass in the Ox direction

v : Displacement of the rotor's center of mass in the Oy direction

θ : Clockwise rotation about the Ox axis

ψ : Clockwise rotation about the Oy axis

δ : Displacement of the ends of the rotor along the Ox and Oy axes

ϕ : Angle representing the offset of the rotor's mass centerline from the line joining the bearings

β : Angle representing the skewed principal axis of inertia relative to the bearing centerline

θ_A : Angle representing the skewed principal axis of inertia relative to the bearing centerline for forced vibration

ψ_A : Angle representing the skewed principal axis of inertia relative to the bearing centerline for forced vibration

ABBREVIATIONS

DOF : Degree of freedom

SDOF : Single degree of freedom

n : Dimensionality of the system

rpm : Revolution per minute

FBD : Free body diagram

LIST OF FIGURES

1. INTRODUCTION

Turbomachinery consists of a rotor, typically with impellers or bladed disks, supported by bearings and rotating within a clearance space. The rotor's motion results in three types of vibrations: torsional, axial, and lateral. Torsional vibration involves the shaft's rotational dynamics and is minimally influenced by the supporting bearings. Axial vibration, concerning the rotor's movement in the axial direction, is usually not problematic. However, lateral vibration, the main focus of this study, refers to the rotor's side-to-side movement and is significantly affected by the bearings. Our study will delve into the fundamental aspects of lateral rotor dynamics in turbomachinery.

Historically, the advent of steam turbines led to frequent issues with blade and rotor vibrations. As steam turbine technology advanced, understanding vibration problems in large-capacity turbines operating under high loads and speeds became crucial. Ensuring the reliability of modern steam turbines necessitates precise determination of vibration characteristics during the design phase and proactive measures against potential damaging vibrations.

In our study, we will concentrate on dynamic analysis, and critical areas in vibration simulation for steam turbines. Utilizing knowledge of elastic systems, rotor dynamics, the Finite Element Method (FEM), and critical speeds, we aim to develop a code to analyze and simulate steam turbine vibrations. This code's objective is to mitigate harmful vibrations, thereby enhancing the reliability and performance of steam turbine designs.

2. BASIC VIBRATION KNOWLEDGE

- **Lateral vibration:** Rotor lateral vibration (sometimes called transverse or flexural vibration) is perpendicular to the axis of the rotor and is the largest vibration component in most high-speed machinery. Understanding and controlling this lateral vibration is important because excessive lateral vibration leads to bearing wear and, ultimately, failure. In extreme cases, lateral vibration also can cause the rotating parts of a machine to come into contact with stationary parts, with potentially disastrous consequences. Lateral vibration is generally caused by lateral forces, the most common of which are unbalance forces that are present in all rotating machines, despite efforts to minimize or eliminate them. In subsequent chapters, we discuss the effects of rotor unbalance and the methods for balancing real machines, but the balance will never be perfect. As in all elastic systems, a machine has natural frequencies of lateral vibration determined by the lateral stiffness and mass distribution of the rotor-bearing foundation system. When the rotational speed - and, hence, the frequency of the out-of-balance forces - is equal to any of these natural frequencies, the vibration response becomes large, and the rotor is considered to be rotating at a critical speed. When a machine is accelerated from rest to its operating speed, it might have to pass through one or more of these critical speeds. For most classes of machine, it is important that it is not permitted to operate at or close to a critical speed for any length of time. Because the rotor can vibrate laterally in two mutually perpendicular directions, the vibrations combine to create an orbit for the rotor motion. If the supporting structure of the bearings of a horizontal rotor has identical stiffness and damping properties in both the horizontal and vertical directions, then this orbit is circular and the bending stresses in the rotor are constant. In many instances, however, the structure supporting the bearings is stiffer in the vertical than in the horizontal direction. In such a situation, the rotor orbit is elliptical and the bending stress in the rotor varies at twice the rotational speed. In the discussion thus far, the role of dissipative or damping forces on the motion has not been mentioned. As in structural dynamics, damping has a major influence close to the resonant frequencies. Although it might be anticipated that damping always tends to reduce vibration, this is not always the case. If the damping forces arise in the supporting structure, then the effects are invariably beneficial and may be treated in much the same way as damping in any structural system. Problems arise, however, when there is damping in the rotor itself. Far from being beneficial, this type of damping can be destabilizing [2]

- **Axial Vibration:** The ultimate function of a jet engine is to produce thrust in the axial direction. A thrust bearing must be fitted to transmit this thrust to the housing and, hence, the aircraft to which it is attached. Without this thrust bearing, the rotor would simply be propelled away from the engine housing and, therefore, would be ineffective! Of course, there is some time-varying fluctuation about the mean level of thrust, which gives rise to axial vibrations of the rotor, with this motion having its own set of resonance frequencies. In contrast to the lateral motion of the rotor, stresses arising from axial vibration are uniform across a complete cross-section of the rotor. There may be cross-coupling between axial and lateral vibrations - for example, in helical and bevel gear meshes.[2]
- **Torsional vibration:** Torsional vibration, or a twisting motion of the rotor about its own axis. In some respects, this is relatively straight-forward to model because bearings and supporting structures have little influence on the natural frequencies. There is also a practical problem: lateral and, to a lesser extent, axial vibrations become obvious by their effects on the machine and its surroundings, enabling the deployment of appropriate effort to resolve developing problems. In complete contrast, torsional problems can go unnoticed without special instrumentation. Furthermore, because little motion is transmitted to components other than the rotor, torsional modes often have low damping. During this undetected phase, however, considerable damage may be caused to a machine.[2]

2.1. Multi-Degree of Freedom Systems

Consider the two-degree-of-freedom system shown in the Figure 4. x_1 and x_2 are measured from

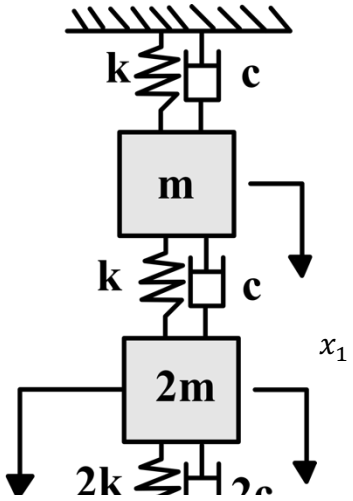

Figure 1: two-degree-of-freedom system

the system's equilibrium position.

Static spring forces cancel with gravity. So, the free body diagrams at an arbitrary instant.

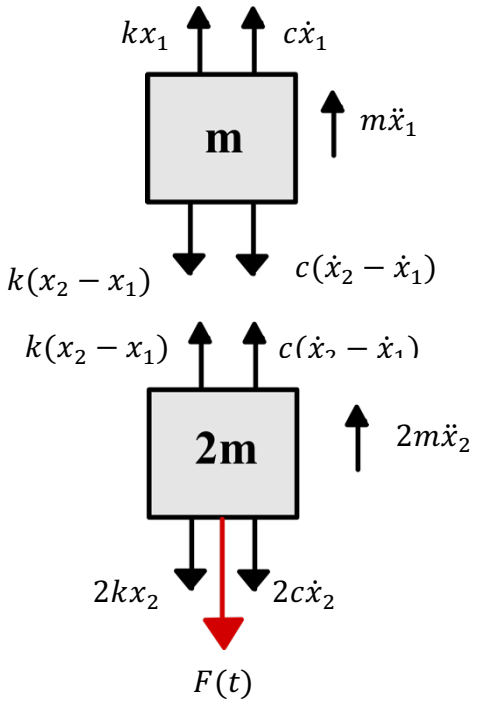

Figure 2: Free body diagram of two-degree-of-freedom system

$$c(\dot{x}_2 - \dot{x}_1) - c\dot{x}_1 + k(x_2 - x_1) - kx_1 - m\ddot{x}_1 = 0$$

$$-c(\dot{x}_2 - \dot{x}_1) - 2c\dot{x}_2 - k(x_2 - x_1) - 2kx_2 + F(t) - 2m\ddot{x}_2 = 0$$

$$c(\dot{x}_2 - \dot{x}_1) - c\dot{x}_1 + k(x_2 - x_1) - kx_1 = m\ddot{x}_1$$

$$-c(\dot{x}_2 - \dot{x}_1) - 2c\dot{x}_2 - k(x_2 - x_1) - 2kx_2 + F(t) = 2m\ddot{x}_2$$

We can arrange the above equations as follows:

$$m\ddot{x}_1 - c(\dot{x}_2 - \dot{x}_1) + c\dot{x}_1 - k(x_2 - x_1) + kx_1 = 0$$

$$2m\ddot{x}_2 + c(\dot{x}_2 - \dot{x}_1) + 2c\dot{x}_2 + k(x_2 - x_1) + 2kx_2 = F(t)$$

or,

$$m\ddot{x}_1 + 2c\dot{x}_1 - c\dot{x}_2 + 2kx_1 - kx_2 = 0$$

$$2m\ddot{x}_2 - c\dot{x}_1 + 3c\dot{x}_2 - kx_1 + 3kx_2 = F(t)$$

The above equations of motion can be written in matrix-vector form as follows:

$$\underbrace{\begin{bmatrix} m & 0 \\ 0 & 2m \end{bmatrix}}_{[M]} \underbrace{\begin{Bmatrix} \ddot{x}_1 \\ \ddot{x}_2 \end{Bmatrix}}_{\{\ddot{x}\}} + \underbrace{\begin{bmatrix} 2c & -c \\ -c & 3c \end{bmatrix}}_{[C]} \underbrace{\begin{Bmatrix} \dot{x}_1 \\ \dot{x}_2 \end{Bmatrix}}_{\{\dot{x}\}} + \underbrace{\begin{bmatrix} 2k & -k \\ -k & 3k \end{bmatrix}}_{[K]} \underbrace{\begin{Bmatrix} x_1 \\ x_2 \end{Bmatrix}}_{\{x\}} = \underbrace{\begin{Bmatrix} 0 \\ F(t) \end{Bmatrix}}_{\{F(t)\}}$$

Where;

$\begin{Bmatrix} \ddot{x}_1 \\ \ddot{x}_2 \end{Bmatrix}$: vector of generalized acceleration

$\begin{Bmatrix} \dot{x}_1 \\ \dot{x}_2 \end{Bmatrix}$: vector of generalized velocities

$\begin{Bmatrix} x_1 \\ x_2 \end{Bmatrix}$: vector of generalized coordinates

$\begin{bmatrix} m & 0 \\ 0 & 2m \end{bmatrix}$: generalized mass or inertia matrix

$\begin{bmatrix} 2c & -c \\ -c & 3c \end{bmatrix}$: generalized damping matrix

$\begin{bmatrix} 2k & -k \\ -k & 3k \end{bmatrix}$: generalized stiffness matrix

$\begin{Bmatrix} 0 \\ F(t) \end{Bmatrix}$: vector of generalized nonconservative external forces (excluding the damper forces)

$$[M]\{\ddot{x}\} + [C]\{\dot{x}\} + [K]\{x\} = \{F(t)\}$$

For a multi-degree-of-freedom system, the equations of motion can be written as follows

$$[M]\{\ddot{q}\} + [C]\{\dot{q}\} + [K]\{q\} = \{Q\}$$

$n =$ number of degrees of freedom (DOF) of the system

$[M]$: $n \times n$ generalized mass or inertia matrix

$[C]$: $n \times n$ generalized damping matrix

$[K]$: $n \times n$ generalized stiffness matrix

$\{\ddot{q}\}$: n-dimensional column vector of generalized accelerations

$\{\dot{q}\}$: n- dimensional column vector of generalized velocities

$\{q\}$: n- dimensional column vector of generalized coordinates

$\{Q\}$: n- dimensional column vector of generalized nonconservative external forces (excluding the damper forces) [3]

2.2. Natural Frequencies and Mode Shapes

Natural frequencies are the frequencies at which undamped vibrations naturally occur. We assumed that the generalized coordinates are synchronous; that is, they vibrate at the same frequency. This is called the normal mode solution.

$$\{q\} = \{X\}e^{i\omega t}$$

$\{X\} = \begin{Bmatrix} X_1 \\ X_2 \\ \vdots \\ X_n \end{Bmatrix}$: Mode shape vector.

Recall:

$$\text{Undamped} \rightarrow [\text{C}] = 0$$

$$e^{i\omega t} = \cos(\omega t) + isin(\omega t), i = \sqrt{-1}$$

Take the derivative of generalized coordinate.

$$\{q\} = \{X\}e^{i\omega t}$$

$$\{\dot{q}\} = i\omega\{X\}e^{i\omega t}$$

$$\{\ddot{q}\} = (i\omega)^2\{X\}e^{i\omega t} = i^2\omega^2\{X\}e^{i\omega t} = -\omega^2\{X\}e^{i\omega t}$$

$$\text{For free vibrations} \rightarrow \{\text{Q}\} = 0$$

$$[M]\{\ddot{q}\} + [C]\{\dot{q}\} + [K]\{q\} = \{Q\}$$

$$[M]\{\ddot{q}\} + [K]\{q\} = 0$$

If we substitute the values we found

$$[M]\left(-\omega^2\{X\}e^{i\omega t}\right) + [K]\left(\{X\}e^{i\omega t}\right) = 0$$

Take the $e^{i\omega t}$ parenthesis,

$$-\omega^2[M]\{X\}e^{i\omega t} + [K]\{X\}e^{i\omega t} = 0$$

$$(-\omega^2[M]\{X\} + [K]\{X\})e^{i\omega t} = 0$$

Exponential term will not be zero. So,

$$(-\omega^2[M]\{X\} + [K]\{X\}) = 0$$

$$\underbrace{(-\omega^2[M] + [K])}_{[A]}\{X\} = 0$$

If $(-\omega^2[M] + [K])$ is non-singular, the only solution of the above equation is the trivial solution; that is, $\{X\} = 0$. For a non-trivial solution to be possible, $(-\omega^2[M] + [K])$ must be singular; that is, $\det(-\omega^2[M] + [K]) = 0$

The nodes are the particles in a system which has zero displacement when the system is vibrating at one of the natural frequencies. These can be determined from the mode shapes. For a two degree of freedom system, there are no nodes associated with the lowest natural frequency and one node associated with the higher natural frequency.[3]

2.3. Finite Element Modeling of Discrete Components

"Consider a discrete system of masses and springs. Figure 4.1 shows a simple Hooke's law spring element, in which the local coordinates are given by the displacement at the ends of the spring. The forces acting on the masses attached to the ends of the spring are shown as Wi and W2 and, for consistency, are positive in the direction of the displacements. From equilibrium, we have that W1 =-W2. Thus, if k is the spring stiffness.

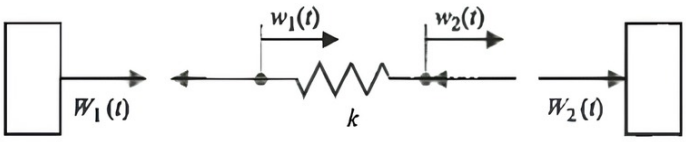

Figure 3: Hook's Law spring

$$W_1 = -W_2 = -k(w_1 - w_2) \tag{1}$$

Therefore, we can express the force produced by changes in the local coordinates w_1 and w_2 Equation (4.1) can be expressed in matrix notation as

$$\begin{Bmatrix} W_1 \\ W_2 \end{Bmatrix} = -k \begin{bmatrix} 1 & -1 \\ -1 & 1 \end{bmatrix} \begin{Bmatrix} w_1 \\ w_2 \end{Bmatrix} = -K_e \begin{Bmatrix} w_1 \\ w_2 \end{Bmatrix} \tag{2}$$

where is called the element stiffness matrix. Equation (4.2) is the standard form for all expressions giving the force due to elastic strain in terms of the displacement. The deformation in the spring is completely specified by the relative displacement of its ends. Using Newton's

second law.

$$m\ddot{\omega} = W \tag{3}$$

where W is the force applied to the mass, m, in the direction ofω . This force arises from the springs as well as from external forces. In Equation (4.3), the mass may be interpreted as a 1 x 1 element mass matrix, M_e; for other types of elements, the size of the matrix is larger.

These spring and mass elements are now assembled to give the complete equations of motion. Consider the system shown in Figure 4.3, consisting of three masses of mass m_1, m_1, and m_3 and four springs of stiffness through k_1 through k_4. The system has three generalized coordinates, q_1, q_2, and q_3, which are the displacements of the three masses. The system also may be excited by external forces on the masses, which are shown by Qi in Figure 4.3. The forces on the masses due to the spring k_2 may be expressed as

$$M\ddot{q} + Kq = Q$$

$$\underbrace{\begin{bmatrix} m_1 & 0 & 0 \\ 0 & m_2 & 0 \\ 0 & 0 & m_3 \end{bmatrix}}_{M} \begin{Bmatrix} \ddot{q_1} \\ \ddot{q_2} \\ \ddot{q_3} \end{Bmatrix} + \underbrace{\begin{bmatrix} k_1 + k_2 + k_4 & -k_2 & -k_4 \\ -k_2 & k_2 + k_3 & -k_3 \\ -k_4 & -k_3 & k_3 + k_4 \end{bmatrix}}_{K} \begin{Bmatrix} q_1 \\ q_2 \\ q_3 \end{Bmatrix} = \begin{Bmatrix} Q_1 \\ Q_2 \\ Q_3 \end{Bmatrix} \tag{4}$$

2.4. Axial Deflection in a Bar

$$\boldsymbol{M_e = \frac{\rho_e A_e l_e}{6}\begin{bmatrix} 2 & 1 \\ 1 & 2 \end{bmatrix}} \textbf{ and } \boldsymbol{K_e = \frac{E_e A_e}{l_e}} \tag{5}$$

$$M_e \begin{Bmatrix} \ddot{\omega}_{e1} \\ \ddot{\omega}_{e2} \end{Bmatrix} + K_e \begin{Bmatrix} \omega_{e1} \\ \omega_{e2} \end{Bmatrix} = \begin{Bmatrix} W_{e1} \\ W_{e2} \end{Bmatrix} \tag{6}$$

$$Q_b = Q_{b1} + Q_{b2} + Q_{b3} \tag{7}$$

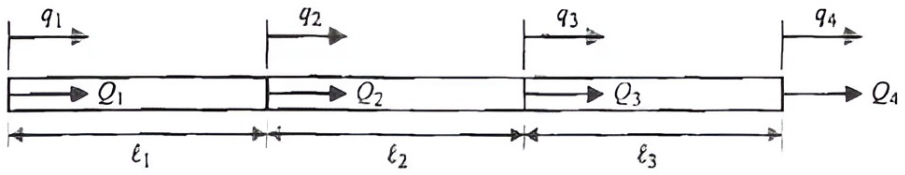

Figure 4: Three element uniform bar

$$= -\frac{EA}{l}\left(\begin{bmatrix} 1 & -1 & 0 & 0 \\ -1 & 1 & 0 & 0 \\ 0 & 0 & 0 & 0 \\ 0 & 0 & 0 & 0 \end{bmatrix} + \begin{bmatrix} 0 & 0 & 0 & 0 \\ 0 & 1 & -1 & 0 \\ 0 & -1 & 1 & 0 \\ 0 & 0 & 0 & 0 \end{bmatrix} + \begin{bmatrix} 0 & 0 & 0 & 0 \\ 0 & 0 & 0 & 0 \\ 0 & 0 & 1 & -1 \\ 0 & 0 & -1 & 1 \end{bmatrix}\right) \begin{Bmatrix} q_1 \\ q_2 \\ q_3 \\ q_4 \end{Bmatrix} \tag{8}$$

$$\frac{\rho_1 A_1 l_1}{6}\begin{bmatrix}1 & -1 & 0 & 0\\ -1 & 2 & -1 & 0\\ 0 & -1 & 2 & -1\\ 0 & 0 & -1 & 1\end{bmatrix}\begin{Bmatrix}\ddot{q}_1\\ \ddot{q}_2\\ \ddot{q}_3\\ \ddot{q}_4\end{Bmatrix} = M_{b1}\ddot{q} \tag{9}$$

where pi is the mass density of the first element. The inertia terms for the other elements may be obtained similarly. Because $q_i = q$ for all I

The inertia term produced by the first element is

$$K = -\frac{EA}{l}\begin{bmatrix}1 & -1 & 0 & 0\\ -1 & 2 & -1 & 0\\ 0 & -1 & 2 & -1\\ 0 & 0 & -1 & 1\end{bmatrix}$$

$$M = M_{b1} + M_{b2} + M_{b3}$$

$$= \frac{\rho Al}{6}\left(\begin{bmatrix}2 & 1 & 0 & 0\\ 1 & 2 & 0 & 0\\ 0 & 0 & 0 & 0\\ 0 & 0 & 0 & 0\end{bmatrix} + \begin{bmatrix}0 & 0 & 0 & 0\\ 0 & 2 & 1 & 0\\ 0 & 1 & 2 & 0\\ 0 & 0 & 0 & 0\end{bmatrix} + \begin{bmatrix}0 & 0 & 0 & 0\\ 0 & 0 & 0 & 0\\ 0 & 0 & 2 & 1\\ 0 & 0 & 1 & 2\end{bmatrix}\right) \tag{10}$$

$$= \frac{\rho Al}{6}\begin{bmatrix}2 & 1 & 0 & 0\\ 1 & 4 & 1 & 0\\ 0 & 1 & 4 & 1\\ 0 & 0 & 1 & 2\end{bmatrix}$$

The equation of motion is obtained as

$$\boldsymbol{M\ddot{q} = Q_b + Q \; or \; M\ddot{q} + Kq = Q}$$

where $Q = \{Q_1 \quad Q_2 \quad Q_3 \quad Q_4\}^T$ is the vector of generalized (external) forces. Thus far, we assume that the bar is free-free; heoce, none of the coordinates is fixed. Suppose that the left end of the bar is fixed so that $q_1 = 0$. From that equation, the equations of motion become

$$\frac{\rho Al}{6}\begin{bmatrix}2 & 1 & 0 & 0\\ 1 & 4 & 1 & 0\\ 0 & 1 & 4 & 1\\ 0 & 0 & 1 & 2\end{bmatrix}\begin{Bmatrix}0\\ \ddot{q}_2\\ \ddot{q}_3\\ \ddot{q}_4\end{Bmatrix} + \frac{EA}{l}\begin{bmatrix}1 & -1 & 0 & 0\\ -1 & 2 & -1 & 0\\ 0 & -1 & 2 & -1\\ 0 & 0 & -1 & 1\end{bmatrix}\begin{Bmatrix}0\\ q_2\\ q_3\\ q_4\end{Bmatrix} = \begin{Bmatrix}Q_1\\ Q_2\\ Q_3\\ Q_4\end{Bmatrix} \tag{11}$$

2.5. Lateral Deflection of a Beam

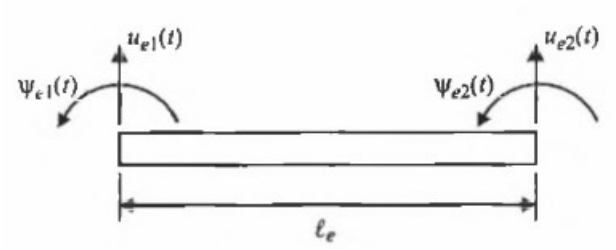

Figure 5: Uniform beam element

The analysis of beam bending may be considered in a manner similar to bar extension. Figure 3 shows a typical element, together with the local coordinates. To ensure the continuity of deflection and slope across the element boundaries, the local coordinates consist of the translations and the rotations at the ends of the element. Euler-Bernoulli Beam Theory develops the element mass and stiffness matrices by approximating the kinetic and strain energies. For the bending motion of a slender beam, the Euler-Bernoulli assumptions hold and the element matrices are

$$M_e = \frac{\rho_e A_e l_e}{420}\begin{bmatrix} 156 & 22l_e & 54 & -13l_e \\ 22l_e & 4{l_e}^2 & 13l_e & -3{l_e}^2 \\ 54 & 13l_e & 156 & -22l_e \\ -13l_e & -3{l_e}^2 & -22l_e & 4{l_e}^2 \end{bmatrix} \tag{12}$$

and

$$K_e = \frac{E_e I_e}{{l_e}^3}\begin{bmatrix} 12 & 6l_e & -12 & 6l_e \\ 6l_e & 4{l_e}^2 & -6l_e & 2{l_e}^2 \\ -12 & -6l_e & 12 & -6l_e \\ 6l_e & 2{l_e}^2 & -6l_e & 4{l_e}^2 \end{bmatrix} \tag{13}$$

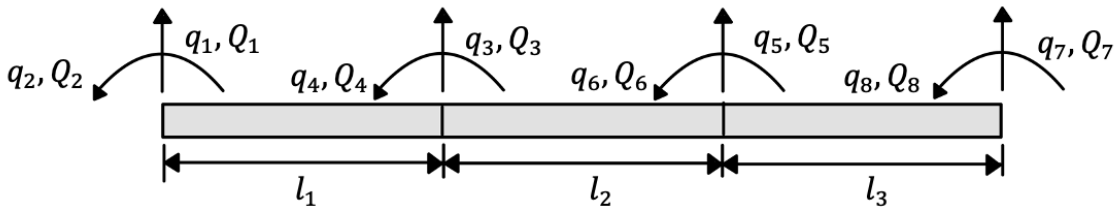

Figure 6: Three element uniform beam

where E_e, I_e, $A_e$and ρ_e are the Young's modulus, second moment of area, cross-sectional area, and mass density of the eth beam element. The assembly of the full mass and stiffness matrices for beam problems is similar to that used for discrete systems and bar elements described

previously. Figure 9 shows the simple example of a beam split into three elements, together with the generalized coordinates for the discretized model. The vector of forces at the four nodes due to the first element is obtained by noting that $q_1 = u_{e1}$, $q_2 = \psi_{e1}$, $q_3 = u_{e2}$, $\rho_4 = \psi_{e2}$. Thus,

$$Q_{b1} = -\frac{E_1 I_1}{{l_1}^3}\begin{bmatrix} 12 & 6l_1 & -12 & 6l_1 & 0 & 0 & 0 & 0 \\ 6l_1 & 4{l_1}^2 & -6l_1 & 2{l_1}^2 & 0 & 0 & 0 & 0 \\ -12 & -6l_1 & 12 & -6l_1 & 0 & 0 & 0 & 0 \\ 6l_1 & 2{l_1}^2 & -6l_1 & 4{l_1}^2 & 0 & 0 & 0 & 0 \\ 0 & 0 & 0 & 0 & 0 & 0 & 0 & 0 \\ 0 & 0 & 0 & 0 & 0 & 0 & 0 & 0 \\ 0 & 0 & 0 & 0 & 0 & 0 & 0 & 0 \\ 0 & 0 & 0 & 0 & 0 & 0 & 0 & 0 \end{bmatrix}\begin{Bmatrix} q_1 \\ q_2 \\ q_3 \\ q_4 \\ q_5 \\ q_6 \\ q_7 \\ q_8 \end{Bmatrix} \tag{14}$$

where Q_{be} denotes the strain force produced by the element number e at the eight generalized coordinates. The element stiffness matrix has been inserted into a 4 x 4 submatrix of the full stiffness matrix. The position of this 4 x 4 matrix is determined by the generalized coordinates specifying the displacement of the element: namely, q_1, q_2, q_3 and q_4. The elastic forces for the other elements and the inertia forces are produced in a similar way.

For a beam with three elements, shown in Figure 9, the total elastic force is

$$\boldsymbol{Q_b = Q_{b1} + Q_{b2} + Q_{b3} = -Kq} \tag{15}$$

Equation (68) highlights that element 1 affects only the first four degrees of freedom, shown diagrammatically in Figure 4.9, in which the shaded areas represent the element stiffness matrices. Element 2 affects only degrees of freedom 3 to 6, and the location of the stiffness matrix for this element is also shown. Similarly, element 3 affects only degrees of freedom 5 to 8.

For a uniform slender beam, $E_i = E$, $I_i = I$, $\rho_i = \rho$, and $l_i = l$ for ail i, and the global stiffness matrix becomes

$$K = \frac{EI}{l^3}\begin{bmatrix} 12 & 6l & -12 & 6l & 0 & 0 & 0 & 0 \\ 6l & 4l^2 & -6l & 2l^2 & 0 & 0 & 0 & 0 \\ -12 & -6l & 24 & 0 & -12 & -6l & 0 & 0 \\ 6l & 2l^2 & 0 & 8l^2 & -6l & 2l^2 & 0 & 0 \\ 0 & 0 & -12 & -6l & 24 & 0 & -12 & 6l \\ 0 & 0 & 6l & 2l^2 & 0 & 8l^2 & -6l & 2l^2 \\ 0 & 0 & 0 & 0 & -12 & -6l & 12 & -6l \\ 0 & 0 & 0 & 0 & 6l & 2l^2 & -6l & 4l^2 \end{bmatrix} \tag{16}$$

The mass matrix is

$$M = \frac{\rho A l}{420}\begin{bmatrix} 12 & 6l_1 & -12 & 6l_1 & 0 & 0 & 0 & 0 \\ 6l_1 & 4{l_1}^2 & -6l_1 & 2{l_1}^2 & 0 & 0 & 0 & 0 \\ -12 & -6l_1 & 12 & -6l_1 & 0 & 0 & 0 & 0 \\ 6l_1 & 2{l_1}^2 & -6l_1 & 4{l_1}^2 & 0 & 0 & 0 & 0 \\ 0 & 0 & 0 & 0 & 0 & 0 & 0 & 0 \\ 0 & 0 & 0 & 0 & 0 & 0 & 0 & 0 \\ 0 & 0 & 0 & 0 & 0 & 0 & 0 & 0 \\ 0 & 0 & 0 & 0 & 0 & 0 & 0 & 0 \end{bmatrix} \tag{17}$$

The equations of motion are then in the standard form

$$\boldsymbol{M\ddot{q} = Q_b + Q \; or \; M\ddot{q} + Kq = Q} \tag{18}$$

where the lengths of the vector of generalized coordinates and the vector of generalized forces are now eight. Thus far, we have assumed that the beam is free-free; thus, none of the coordinates is fixed. Suppose that both ends of the beam are pinned, which implies that $q_1 = q_7 = 0$. The mass and stiffness matrices for this problem are obtained from Equations (70) and (71) by deleting the first and seventh rows and columns from the mass and stiffness matrices for the free-free case. Thus, for example

$$K = \frac{EI}{l^3}\begin{bmatrix} 4l^2 & -6l & 2l^2 & 0 & 0 & 0 \\ -6l & 24 & 0 & -12 & 6l & 0 \\ 2l^2 & 0 & 8l^2 & -6l & 2l^2 & 0 \\ 0 & -12 & -6l & 24 & 0 & 6l \\ 0 & 6l & 2l^2 & 0 & 8l^2 & 2l^2 \\ 0 & 0 & 0 & 6l & 2l^2 & 4l^2 \end{bmatrix} \tag{19}$$

The rows deleted from the unconstrained equation of motion give the reaction force required on the pinned constraints to maintain the zero displacement. The process may be repeated if other boundary conditions are required. For example, if the left-hand end were fixed, giving the model of a cantilever beam, then $q_1 = q_2 = 0$."[2]

3. Journal Bearings

Fluid (oil) film bearings are the most used method for supporting turbomachinery. Naturally, rolling element bearings are also utilized in numerous gas turbine applications. However, we will address the influence of journal bearings on the rotor's dynamic behavior later in this paper. The term "journal" refers to the section of the shaft that is supported by a bearing. Engineers involved in the design and operation of bearings for turbomachinery must understand the impact bearings have on the rotor's dynamic behavior.

When the shaft is stationary (at zero speed), it rests at the bottom of the clearance space. As the rotor accelerates, it begins to "climb" onto the inner surface of the bearing. The convergent wedge formed between the rotating shaft and the inner surface of the bearing housing functions as a “pump,” pushing the oil beneath the shaft. This action lifts the shaft, and at operating speed, the shaft settles into an equilibrium position. These stages are illustrated in Figure 7.

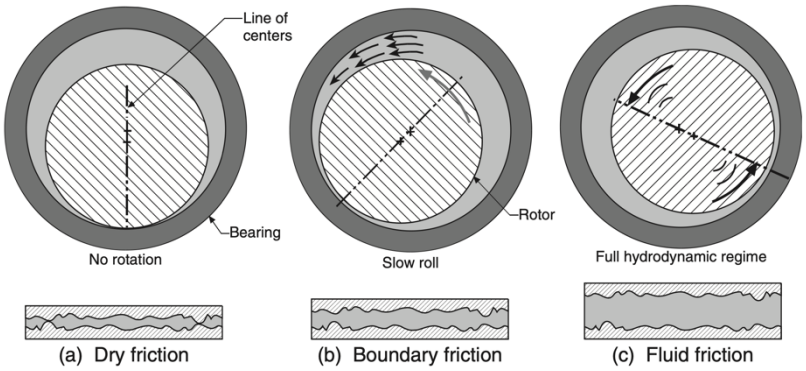

Figure 8: Motion of the shaft in the bearing from rest to speed[5]

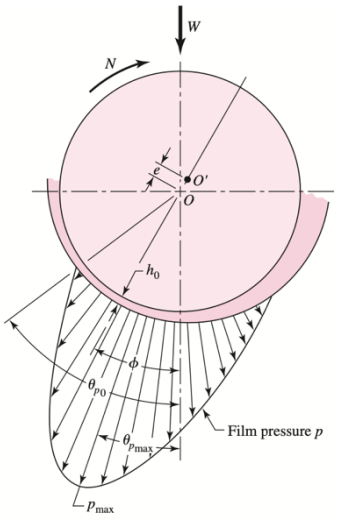

Figure 7: Pressure profile in a simple sleeve bearing[4]

The rotating shaft is supported by a thin film of oil. The thin oil film that is "squeezed" between the shaft and the housing, generates a pressure that supports the rotor weight. Figure 5 shows the pressure profile of a simple sleeve bearing. The distance between the geometric center of the bearing and the center of the rotating shaft is known as eccentricity (e). [1]

3.1. Motion of the Shaft in the Bearing

"Figure 9 shows the schematic of a simple type of journal bearing (also known as sleeve bearing). The shaft rotates in the clearance space (exaggerated) of the bearing as shown. The clearance is usually about 1.5 mils/inch of the journal diameter. Typically for a 4-in. journal diameter, the bearing would have a clearance of 6 mils. When the shaft rotates in the bearing clearance space, it has two kinds of motions.

- The first motion is the rotation or the spin of the shaft. This is the same as the running speed of the shaft.
- The second type of motion is the precession which is the rotation of the center of the shaft with respect to the geometric center of the bearing. (An analogy would be the motion of the earth which rotates about its axis and also revolves round the sun) This precession (in rotor dynamic terminology) is more commonly known as whirl. This whirl motion is further classified as forward whirl (shown in Figure 9) and backward whirl. Forward whirl is the motion in which the center of the shaft moves in the same direction as the rotation of the shaft. The backward whirl is the motion in which the center of the shaft moves in the opposite direction as the rotation of the shaft. In general, the whirl orbit is elliptical."[1]

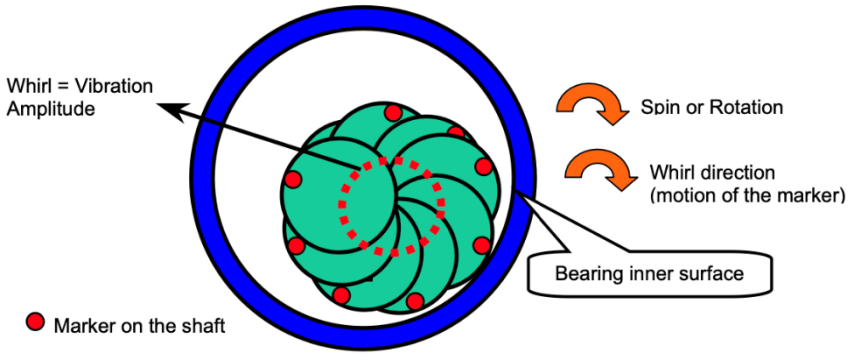

Figure 9:Example of forward whirl in the bearing clearance space [1]

3.2. Bearing stiffness and damping coefficients

When the shaft is not rotating it is resting at the bottom of the clearance space in the bearing. With the clearance space filled with oil, as the shaft starts to rotate, it acts as a "pump", "pushing" the oil underneath itself! This generates the lift of the shaft. At any constant rotating speed, the center of the shaft is located away from the geometric center of the bearing as shown in Figure 5. This is known as the eccentricity of the journal. The oil "wedge" supports the shaft. The properties associated with the oil film are stiffness and damping. These are inherent properties of the oil and are a function of oil type, viscosity, temperature, etc. For analytical purposes the stiffness and damping are oriented towards the horizontal and vertical axes – hence, the bearing is said to have a horizontal stiffness and vertical stiffness (same for the damping). The horizontal stiffness is indicated by Kxx and the vertical stiffness by Kyy.

Similarly the damping is indicated as C_{xx} and C_{yy}. To complicate, real life, things, because the oil film is continuous around the shaft, there exist components of the stiffness and damping in the x-y direction also!

The role played by this cross-coupled stiffness (Kxy) is very important in the understanding of the stability of rotor-bearing systems.[1]

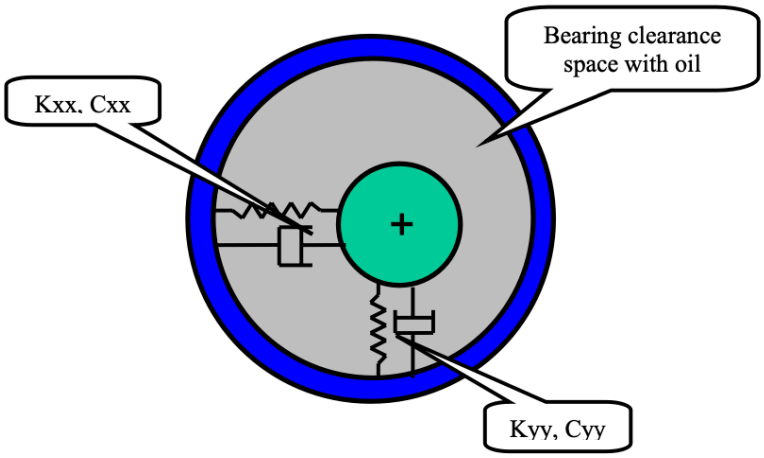

Figure 10:A simple journal bearing geometry[1]

3.3. Hydrodynamic Journal Bearings

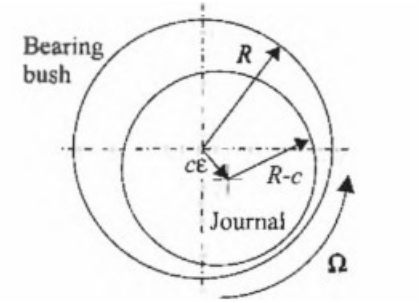

Figure 11: Fluid-bearing geometry. R is the bearing radius (D /2), c is the bearing clearance, and ε is the eccentricity.[2]

The hydrodynamic bearing, often called the oil or fluid film bearing, is extensively used in large rotating machines because of its high load-carrying capacity. It consists of a bearing bush in which the shaft or journal rotates, as shown in Figure 7. The bush has an internal diameter that is slightly greater than the diameter of the journal, thereby providing a clearance space between the bush and the journal, which is typically between 0.1 and 0.2 percent of the journal diameter. Oil is fed into the clearance space through one or more holes or grooves and, due to its viscosity and the rotation of the journal, it is swept circumferentially to create an oil film between the journal and bush. The oil eventually leaves the bearing by leakage from the ends.

Most bearings are designed to operate with the ratio between the journal displacement and the radial clearance of about 0.6-0.7. This ratio is called the eccentricity, ε. When $\varepsilon = 1$, the oil film has zero thickness at one point and the bearing surfaces are in contact.

Let us assume that,

- the flow is laminar, and Reynolds's equation applies
- the bearing is very short, so that L /D 1, where L is the bearing length and D is the bearing diameter, which means that the pressure gradients are much larger in the axial than in the circumferential direction
- the lubricant pressure is zero at the edges of the bearing
- the bearing is operating under steady running conditions
- the lubricant properties do not vary substantially throughout the oil film
- the shaft does not tilt in the bearing

The radial and tangential forces, f_r and f_t

$$f_r = -\frac{D\Omega\eta L^3\varepsilon^2}{2c^2(1-\varepsilon^2)^2} \quad and \; f_t = -\frac{\pi D\Omega\eta L^3\varepsilon}{8c^2(1-\varepsilon^2)^{\frac{3}{2}}} \tag{20}$$

Where η is the absolute viscosity of the oil, Ω is the speed of rotation, c is the bearing radial clearance, L, D, and ε are defined previously.

The magnitude of the resultant force f is

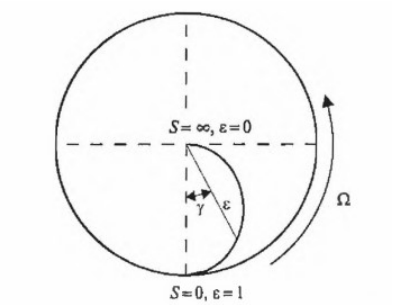

Figure 12: Locus o f the equilibrium position of the journal, assuming short-bearing theory.[2]

$$f = \sqrt{f_r^2 + f_t^2} = \frac{\pi D\Omega\eta L^3\varepsilon}{8c^2(1-\varepsilon^2)^{\frac{3}{2}}}\left(\left(\frac{16}{\pi^2}-1\right)\varepsilon^2+1\right)^{\frac{1}{2}} \tag{21}$$

If the magnitude of this load is known, then the bearing eccentricity may be obtained by rearranging Equation (5.82) to give the following quartic equation in ε^2:

$$\varepsilon^8 - 4\varepsilon^6 + \left(6 - S_s^2(16-\pi^2)\right)\varepsilon^4 - (4+\pi^2 S_s^2)\varepsilon^2 + 1 = 0 \tag{22}$$

Where

$$S_s = \frac{D\Omega\eta L^3}{8fc^2} \tag{23}$$

is called the modified Sommerfeld number or the Ocvirk number and is known for a particular speed, load, and oil viscosity.

A more general nondimensional parameter is called the Sommerfeld number or duty parameter, S, which is typically defined as

$$S = \frac{S_s}{\pi}\left(\frac{D}{L}\right)^2 = \frac{D^3\Omega\eta L}{8\pi f c^2} \tag{24}$$

The force f must be in the direction of the force applied to the bearing. This direction is given by $\tan\gamma = f_t/f_r$. Thus,

$$\tan\gamma = \frac{\pi\sqrt{1-\varepsilon^2}}{4\varepsilon} \tag{25}$$

4. Jeffcott rotor

"This model is called the Jeffcott rotor named after the English dynamicist who first used the model in 1919 to analyze the synchronous response of high-speed rotating machines to rotor imbalance. It con- sists of a massive unbalanced disk mounted midway between the bearing supports on a flexible shaft of negligible mass. The bearings are rigidly supported, and viscous damping acts to oppose absolute motions of the disk.

Jeffcott's analysis explained how the rotor whirl amplitude becomes a maximum value at the critical speed but diminishes as the critical speed is exceeded due to the critical speed inversion of the imbalance."[5]

4.1. Rotor Supported on Rigid Supports

"Let us assume that the mass is concentrated at the midspan. The bearings are assumed to be rigid supports. Thus the rotor can be assumed to be simply supported. Using the theory of beams, the stiffness of the simply supported beam can be written as,

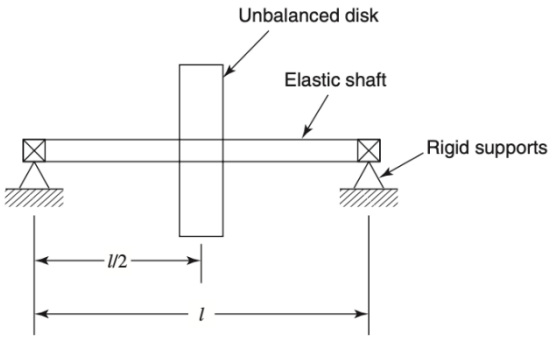

Figure 13: Jeffcott Rotor[5]

$$\frac{48EI}{l^3} = \frac{48E(\pi d^4)}{64\,l^3}$$

where, l = "length" refers to the bearing span (axial distance between the bearing centerlines) and d = diameter of the shaft.

For natural frequency, we obtain,

$$\omega_n = \sqrt{\frac{k}{m}} = \sqrt{\frac{48E(\pi d^4)}{64\ l^3\ m}}$$

and thus proportional to $d^2/ l^{1.5}$. Then for rotors with small (slender) shafts with large external masses the critical frequency is directly proportional to the square of the diameter of the shaft and inversely proportional to the 1.5 power of the bearing span. This important relationship can be used to physically understand the effects of the design changes to these machines.

For distributed system, the derivation of stiffness becomes a little more complicated. If we assume no (or negligible) external mass on the shaft of diameter d and length l, and the shaft mass m, the equation for natural frequency can be written as,

$$\omega_n = \sqrt{\frac{k_{eq}}{m}} = \sqrt{\frac{\pi^4\ E\ (\pi d^4)}{64\ l^3} \times \frac{4\ \pi^4 E}{\rho\ \pi\ d^2\ l}} = \sqrt{\left(\frac{\pi^4 E}{16\rho}\right)\frac{d^2}{l^4}} = f\left(\frac{d}{l^2}\right)$$

In other words, for rotors with small external masses compared to the shaft, the natural frequency is directly proportional to the diameter and inversely proportional to the second power of the length. This important relationship also can be used to physically understand the effects of the design changes to the machine.

In both cases as the diameter of the shaft increases the natural frequency increases and as the bearing span increases the natural frequency decreases."[1]

4.2. Rotor Supported on Flexible Supports

"In the real world, the support is not infinitely rigid. There is a finite amount of stiffness that a journal bearing provides at the supports. Figure 11 shows the rotor supported on actual bearings. The bearing stiffness and damping are given by K_b and C_b respectively.

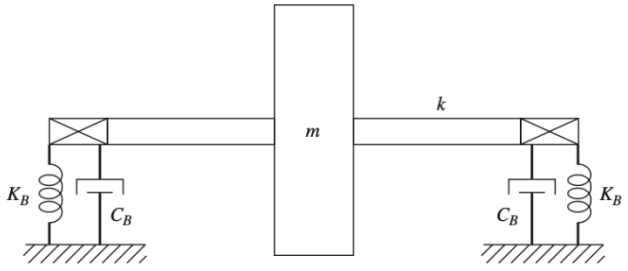

Figure 14: Jeffcott rotor modified to include damped flexible bearing supports. [5]

Adding the bearing stiffness in series with the shaft stiffness, reduces the effective stiffness as in the equation,

$$\frac{1}{K_{eff}} = \frac{1}{2K_B} + \frac{1}{K_s}$$

Hence, using the equation for natural frequency $\omega_n = \sqrt{K_{eff}/m}$, we can see that adding the bearing stiffness, reduces the natural frequency of the system!"[1]

5. ROTOR DYNAMICS

5.1. Dynamics of a Rigid Rotor on Flexible Supports

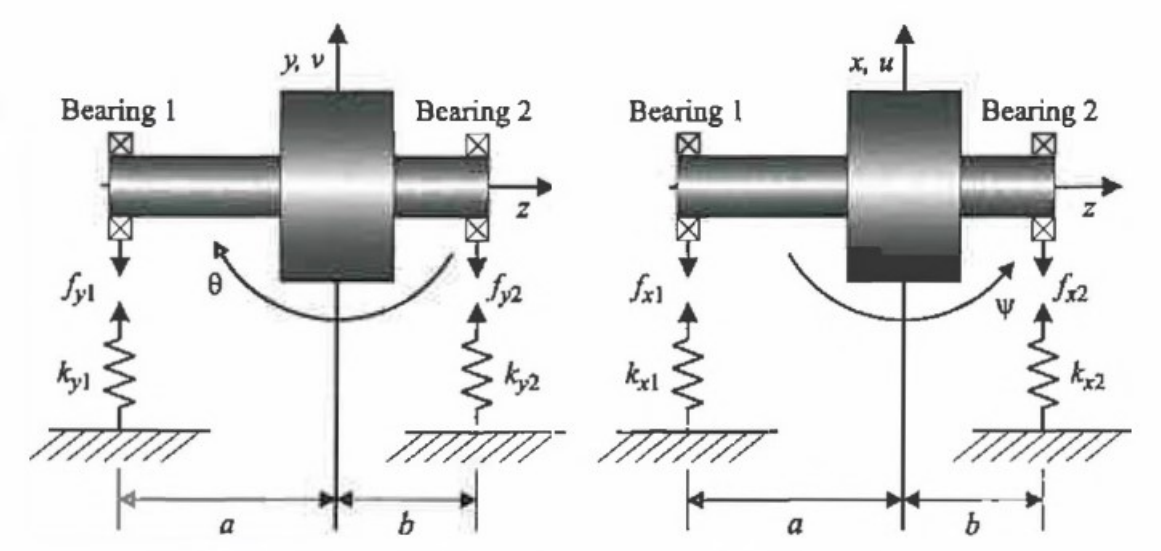

Figure 15: Free-body diagram for a rigid rotor on flexible supports.[2]

The rotor has four degrees of freedom because it can translate in the directions Ox and Oy and it also can rotate about these axes. Practitioners often term the translation and rotation as bounce and tilt motion, respectively. We have chosen to describe the movement of the rotor in terms of the displacements of its center of mass in the directions Ox and Oy, u and v, respectively, and the clockwise rotations about Ox and Oy, θ and ψ, respectively. This is not the only set of coordinates that can be used to describe the displacements of the rotor. For example, we can use the displacements of the ends of the rotor along the Ox and Oy axes; again, we would have four coordinates. The resultant equations would be different but the solutions of both sets of equations would have the same physical meaning.[2]

Applying Newton's second law of motion to the free rotor, we have:

$$Forces\ acting\ on\ rotor\ in\ x\ direction:\ -f_{x1} - f_{x2} = m\ddot{u}$$

$$Forces\ acting\ on\ rotor\ in\ y\ direction:\ -f_{y1} - f_{y2} = m\ddot{v}$$

$$Moments\ acting\ on\ rotor\ in\ \theta\ direction:\ -af_{y1} - bf_{y2} = I_d\ddot{\theta} + I_p\Omega\dot{\psi}$$

$$Moments\ acting\ on\ rotor\ in\ \psi\ direction:\ af_{x1} - bf_{x2} = I_d\ddot{\psi} - I_p\Omega\dot{\theta}$$

Let us assume that the displacements of the rotor from the equilibrium position are small, which is the case in practice (unless there is a catastrophic failure of our rotor-bearing system). This assumption means that the rotations θ and ψ are small; hence, we can replace sin(θ) by θ and sin(ψ) by ψ. Furthermore, we assume that the spring supports are linear, and that Hooke's law applies. Then, assuming no elastic coupling between the Ox and Oy directions

$$f_{x1} = k_{x1}\delta = k_{x1}(u - a\sin\psi) \approx k_{x1}(u - a\psi)$$

Applying this argument to each of the forces, we have

$$f_{x1} = k_{x1}(u - a\psi)$$

$$f_{x2} = k_{x2}(u + b\psi)$$

$$f_{y1} = k_{y1}(v + a\theta)$$

$$f_{y2} = k_{y2}(v - b\theta)$$

Substituting these forces into equations of motion and rearranging gives

$$m\ddot{u} + k_{x1}(u - a\psi) + k_{x2}(u + b\psi) = 0$$

$$m\ddot{v} + k_{y1}(v + a\theta) + k_{y2}(v - b\theta) = 0$$

$$I_d\ddot{\theta} + I_p\Omega\dot{\psi} + ak_{y1}(v + a\theta) - bk_{y2}(v - b\theta) = 0$$

$$I_d\ddot{\psi} - I_p\Omega\dot{\theta} - ak_{x1}(u - a\psi) + bk_{x2}(u + b\psi) = 0$$

These equations can be further rearranged to give:

$$m\ddot{u} + (k_{x1} + k_{x2})u + (-ak_{x1} + bk_{x2})\psi = 0$$

$$m\ddot{v} + (k_{y1} + k_{y2})v + (ak_{y1} - bk_{y2})\theta = 0$$

$$I_d\ddot{\theta} + I_p\Omega\dot{\psi} + (ak_{y1} - bk_{y2})v + (a^2k_{y1} + b^2k_{y2})\theta = 0$$

$$I_d\ddot{\psi} - I_p\Omega\dot{\theta} + (-ak_{x1} + bk_{x2})u + (a^2k_{x1} + b^2k_{x2})\psi = 0$$

Letting

$$k_{xT} = k_{x1} + k_{x2}, \qquad k_{yT} = k_{y1} + k_{y2}$$

$$k_{xC} = -ak_{x1} + bk_{x2}, \qquad k_{yC} = -ak_{y1} + bk_{y2}$$

$$k_{xR} = a^2k_{x1} + b^2k_{x2}, \qquad k_{yR} = a^2k_{y1} + b^2k_{y2}$$

where the subscripts T, C, and R have been chosen to indicate translational, coupling between displacement and rotation, and rotational stiffness coefficients.

We can include the effect of damping in the supports. We now consider the effect of viscous damping in the bearings. Assuming that a viscous damper is placed in parallel with each spring element supporting the bearing, the forces $f_{x1}, f_{x2}, f_{y1}, f_{y2}$ of Equation now become:

$$f_{x1} = k_{x1}(u - a\psi) + c_{x1}(\dot{u} - a\dot{\psi})$$

$$f_{x2} = k_{x2}(u + b\psi) + c_{x2}(\dot{u} + b\dot{\psi})$$

$$f_{y1} = k_{y1}(v + a\theta) + c_{y1}(\dot{v} + a\dot{\theta})$$

$$f_{y2} = k_{y2}(v - b\theta) + c_{y2}(\dot{v} - b\dot{\theta})$$

where c is the viscous-damping coefficient and is defined as the force required to produce a unit velocity across the damping element. Let

$$c_{xT} = c_{x1} + c_{x2}, \qquad c_{yT} = c_{y1} + c_{y2}$$

$$c_{xC} = -ac_{x1} + bc_{x2}, \qquad c_{yC} = -ac_{y1} + bc_{y2}$$

$$c_{xR} = a^2c_{x1} + b^2c_{x2}, \qquad c_{yR} = a^2c_{y1} + b^2c_{y2}$$

Using these definitions, and rearranging these equations gives

$$m\ddot{u} + c_{xT}\dot{u} + c_{xC}\dot{\psi} + k_{xT}u + k_{xC}\psi = 0$$

$$m\ddot{v} + c_{yT}\dot{v} - c_{yC}\dot{\theta} + k_{yT}v - k_{yC}\theta = 0$$

$$I_d\ddot{\theta} + I_p\Omega\dot{\psi} - c_{yT}\dot{v} + c_{yR}\dot{\theta} - k_{yC}v + k_{yR}\theta = 0$$

$$I_d\ddot{\psi} - I_p\Omega\dot{\theta} + c_{xC}\dot{u} + c_{xR}\dot{\psi} + k_{xC}u + k_{yR}\psi = 0$$

5.2. Modeling Out-of-Balance Forces and Moments

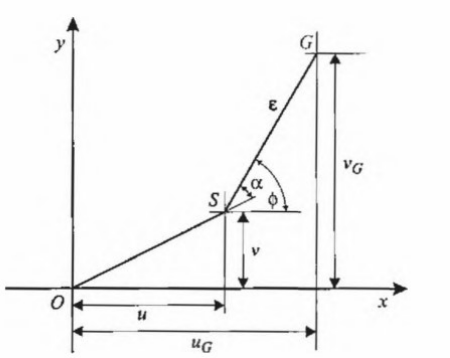

Figure 16: Instantaneous position of bearing centerline S and rotor mass center G.[2]

from Figure above, it is shown that:

$$u_G = u + \varepsilon \cos\phi$$

$$v_G = v + \varepsilon \sin\phi$$

Differentiating these equations twice with respect to time and noting that e is constant gives:

$$\ddot{u}_G = \ddot{u} + \varepsilon(-\dot{\phi}^2 \cos\phi - \ddot{\phi} \sin\phi)$$

$$\ddot{v}_G = \ddot{v} + \varepsilon(-\dot{\phi}^2 \sin\phi - \ddot{\phi} \cos\phi)$$

In deriving the previous equation, we have not restricted the analysis to the case of a rotor spinning with a constant angular velocity. If we now introduce this simplification, then at a constant speed of rotation, Ω, $\dot{\phi} = \Omega$ and $\ddot{\phi} = 0$. Thus,

$$\ddot{u}_G = \ddot{u} - \varepsilon\Omega^2 \cos\Omega t$$

$$\ddot{v}_G = \ddot{v} - \varepsilon\Omega^2 \sin\Omega t$$

Substituting for $\ddot{u}_G$ and $\ddot{v}_G$ and rearranging the equations of motion gives

$$m\ddot{u} + c_{xT}\dot{u} + c_{xC}\dot{\psi} + k_{xT}u + k_{xC}\psi = m\varepsilon\Omega^2 \cos\Omega t$$

$$m\ddot{v} + c_{yT}\dot{v} - c_{yC}\dot{\theta} + k_{yT}v - k_{yC}\theta = m\varepsilon\Omega^2 \sin\Omega t$$

$$I_d\ddot{\theta} + I_p\Omega\dot{\psi} - c_{yT}\dot{v} + c_{yR}\dot{\theta} - k_{yC}v + k_{yR}\theta = 0$$

$$I_d\ddot{\psi} - I_p\Omega\dot{\theta} + c_{xC}\dot{u} + c_{xR}\dot{\psi} + k_{xC}u + k_{yR}\psi = 0$$

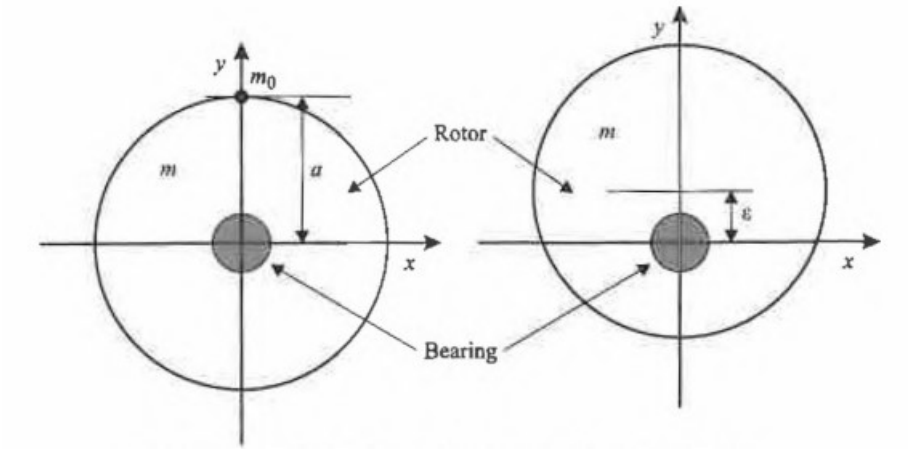

Figure 17: Models of out of balance causing a lateral force[2]

we imagine that the out-of-balance force arose because the total mass of the rotor is offset from the line joining the bearings by a small amount e. This is shown in the right-hand diagram in above Figure. In such a case, the out-of-balance force is given by

$$f = m\varepsilon\Omega^2$$

where m is the total mass of the rotor. This force appears on the right-hand side of above Equation, resolved into two components. The alternative approach assumes that the original rotor mass center is coincident with the bearing centerline but that an extra (insignificant) mass, m_0, is fixed to the rotor a distance a from the bearing centerline. The added mass, m_0, is negligible compared to the rotor mass. This model is shown in the left-hand diagram in above Figure. The lateral acceleration of mass m_0 is $a\Omega^2$ and the resultant force is

$$f = m_0\varepsilon\Omega^2$$

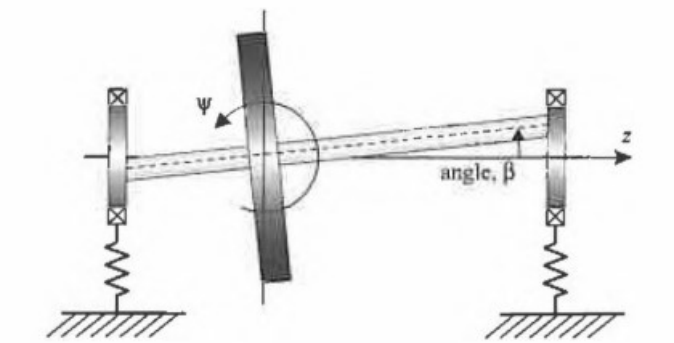

From Figure[2] above:

$$\theta_A = \theta - \beta \sin \Omega t$$

$$\psi_A = \psi + \beta \cos \Omega t$$

Thus,

$$\dot{\theta}_A = \dot{\theta} - \beta\Omega \cos \Omega t$$

$$\dot{\psi}_A = \dot{\psi} - \beta\Omega \sin \Omega t$$

and

$$\ddot{\theta}_A = \ddot{\theta} - \beta\Omega^2 \sin \Omega t$$

$$\ddot{\psi}_A = \ddot{\psi} - \beta\Omega^2 \cos \Omega t$$

Substituting $\dot{\theta}_A, \ddot{\theta}_A, \dot{\psi}_A, \ddot{\psi}_A$ into equations of motion under a forced vibration. the effect of a skewed principal axis of inertia relative to the bearing centerline is to cause out-of-balance moments to act on the system. The term swash is often used by engineers to describe an angle between the shaft and the normal to a disk.[2]

$$m\ddot{u} + c_{xT}\dot{u} + c_{xC}\dot{\psi} + k_{xT}u + k_{xC}\psi = 0$$

$$m\ddot{v} + c_{yT}\dot{v} - c_{yC}\dot{\theta} + k_{yT}v - k_{yC}\theta = 0$$

$$I_d\ddot{\theta} + I_p\Omega\dot{\psi} - c_{yT}\dot{v} + c_{yR}\dot{\theta} - k_{yC}v + k_{yR}\theta = -(I_d - I_p)\beta\Omega^2 \sin \Omega t$$

$$I_d\ddot{\psi} - I_p\Omega\dot{\theta} + c_{xC}\dot{u} + c_{xR}\dot{\psi} + k_{xC}u + k_{yR}\psi = (I_d - I_p)\beta\Omega^2 \cos \Omega t$$

Forward- and Backward- Whirl Orbits

Last section demonstrates that for a particular mode, the orbit of the nodes on a rigid rotor on anisotropic supports is elliptical and gives a method to calculate the dimensions and orientation of the ellipse. It is now shown that the unbalanced response of a rigid rotor also whirls either forward or backward in an elliptical orbit. The direction of the orbit is calculated using the methods in the last section. Elliptical orbits, unlike forward circular orbits, cause alternating stresses and, hence, the potential to cause fatigue, particularly in flexible shafts. The practical implications of these alternating stresses are greater for backward-whirling orbits. We now calculate the unbalance response and orbits of a rigid rotor at different rotational speeds.[2]

Complex Rotor Models

We discuss the FE modeling of the rotor and bearing and determines the free response. We now consider the forced response of complex rotor models to various forms of excitation using FEA. Here, we focus on the derivation of the vector of forces acting on the system and an

interpretation of the resulting responses.

Once the system response is determined at each node in terms of the displacements in the x and y directions, then the operating deflection shape and the orbit of the rotor at a particular node can be constructed. We also can determine the size of the major and minor axes of the elliptical orbit and the direction of rotor whirl around the orbit at each node using the methods described in the last section. Within a response, all the nodes are often whirling either forward or backward; however, part of a rotor may be executing forward whirl and part may be executing backward whirl. We now calculate the unbalance response and orbits of a flexible rotor at several rotational speeds.

Response of Rotors to Out-of-Balance Forces and Moments

The equation of motion for the free vibration of a multiple degrees of freedom rotor-bearing system is below:

$$\boldsymbol{M\ddot{q} + \Omega G\dot{q} + C\dot{q} + Kq = 0}$$

If there is a difference between the equilibrium position and the mass centerline of the rotor in any plane of rotation along the rotor, then out-of-balance forces and moments arise in that plane when the rotor spins. If we let the differences between the equilibrium position and the rotor center of mass at various locations along the rotor be $\boldsymbol{q_\varepsilon}$, and then replace by $\boldsymbol{q + q_\varepsilon}$ in the inertia and gyroscopic terms the equation of motion for the free vibration of a multiple degrees of freedom rotor-bearing system is below:

$$\boldsymbol{M(\ddot{q} + \ddot{q}_\varepsilon) + \Omega G(\dot{q} + \ddot{q}_\varepsilon) + C\dot{q} + Kq = 0}$$

Thus,

$$\boldsymbol{M\ddot{q} + \Omega G\dot{q} + C\dot{q} + Kq = -M\ddot{q}_\varepsilon - \Omega G\dot{q}_\varepsilon}$$

the excitation and response is harmonic, $\boldsymbol{\ddot{q}_\varepsilon = -\Omega^2 q_\varepsilon}$ hence,

$$\boldsymbol{M\ddot{q} + \Omega G\dot{q} + C\dot{q} + Kq = -\Omega^2 Mq_\varepsilon - \Omega G\dot{q}_\varepsilon}$$

Formal Definitions of Critical Speeds

We state that a critical speed is a rotational speed of a machine at which some combination of vibration displacements and/or forces reaches a (local) maximum. For most practical purposes, this is a perfectly workable definition. However, there are some problems with this definition, as follows:

• This definition depends on the distribution of forcing (usually unbalance) applied. In

analyzing machine dynamics, a clear distinction is usually drawn between system properties such as stiffness, damping, and mass (which are features of a particular design) and the forcing applied (which is normally designed to be near zero). Most forcing comes about as a result of imperfections in the machine construction; the level of these imperfections may be reduced but not eliminated by the design.

- Depending on which vibration quantities are selected for consideration as well as weighting attached to each one, different critical speeds are detected. Also, in systems with general (i.e., nonproportional) damping, the peaks in the response may occur at slightly different rotational speeds at different degrees of freedom.
- Local maxima in some vibration measurements may exist at speeds that are by no means critical in that they are neither fundamental characteristics of the system nor speeds at which the vibration of the machine is likely to reach problematic levels.

For these reasons, a more useful definition of critical speeds is that it is a rotational speed of a machine at which one of the frequency components of forcing coincides with a natural frequency of the system.[2]

Features of Critical Speeds

The critical speeds of rotating systems have a number of important features, many of which are similar to the features of natural frequencies. In a cyclically symmetrical rotor with isotropic support characteristics, the critical speeds occur in pairs, each corresponding to a set of four eigenvalues. These critical speeds separate due to bearing and support anisotropy and gyroscopic effects. Often, when engineers discuss the first critical speed of a machine, they are referring to a pair of critical speeds, corresponding to four roots of the characteristic equation.[2]

Mode Shapes Associated with Critical Speeds

We computed the mode shapes or eigenvectors for a constant rotor speed. It is obvious that the mode shape corresponding to a critical speed is important in determining how the rotor system might vibrate when the critical speed is excited. This mode shape is calculated easily by setting the rotor speed equal to the critical speed and computing the right eigenvector[2].

Maps of Critical Speeds and Mode Shapes

Frequently, in the design of machines, some of the parameters that directly affect the rotor dynamics of the machine are not accurately known. Bearing-support stiffness is one such parameter. However, modeling is invariably an expensive exercise. If machine builders can determine that they do not need to model bearing-support stiffness, for example, in any better way than simply recalling an empirical value, this is a positive outcome. Bearing-support stiffness is a particularly relevant example of such a variable parameter because this quantity may depend not only on the design and manufacture of a particular machine, it also can depend strongly on the way in which that machine is mounted. Maps of critical speed and mode shapes enable an engineer to obtain rapidly an impression of how the uncertainty in one of the parameters affects the behavior of the machine. The most relevant concern is that the parameter cannot assume a value that causes one of the machine critical speeds to occur at an undesirable part of the running range of speeds.[2]

6. RESULTS and DISCUSSION

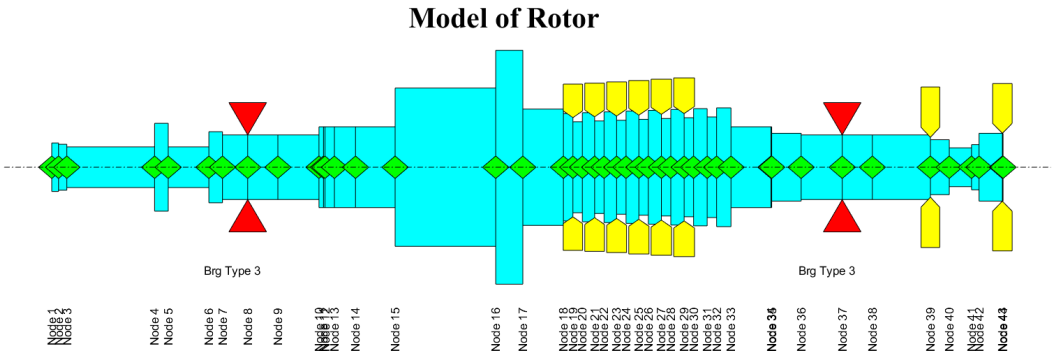

Figure 18: Model of Rotor

Based on the information obtained from the reference source [6] and considering the shaft, bearing and disk data in Tables 1, 2, 3, 4 and 5 (Appendix B) we modeled the rotor using Rotor Dynamic Software V2, as shown in Figure 18 using the relevant MATLAB code. During the modeling process of the rotor, a non-uniform shaft design was created, consisting of 43 elements and 44 nodes of different lengths and diameters. Bearing Type 3 was created by using the stiffness (kxx, kyy) and damping (cxx, cyy) values read from the table at 3000 rpm for the First and Second Bearings. Finally, while creating the disks, Disk Type 2 was created by using the mass, diameter and polar inertia values of a total of 8 disks. So, we used the real rotor information to model the rotor in a basic way in MATLAB.

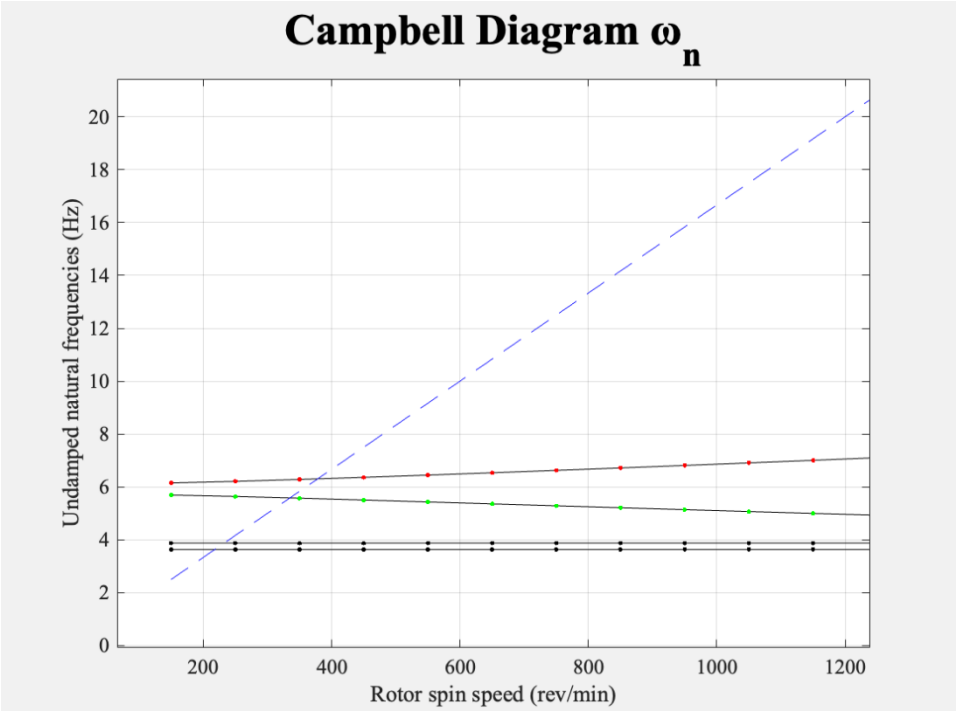

Figure 19: The Campbell diagram for a rigid rotor for natural frequencies. The dashed line represents $\omega = \Omega$ FW indicates forward whirl and BW indicates backward whirl

As seen in Figure 19 in the Campbell Diagram, the values where the dashed lines intersect with the horizontal lines give us 4 natural frequency values.

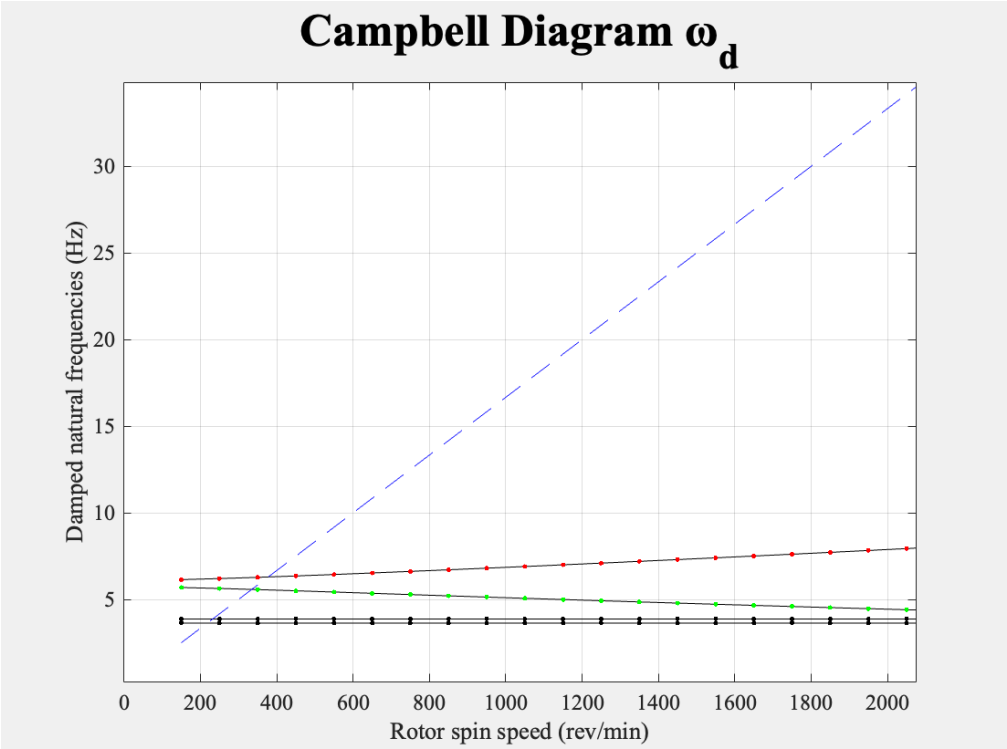

Figure 20: The Campbell diagram for a rigid rotor for natural frequencies. The dashed line represents $\omega = \Omega$ FW indicates forward whirl and BW indicates backward whirl

As seen in Figure 20, the values where the dashed lines intersect with the horizontal lines give us four damping frequency values. The natural frequencies and damping frequencies are quite similar. This is because the damping ratio is small.

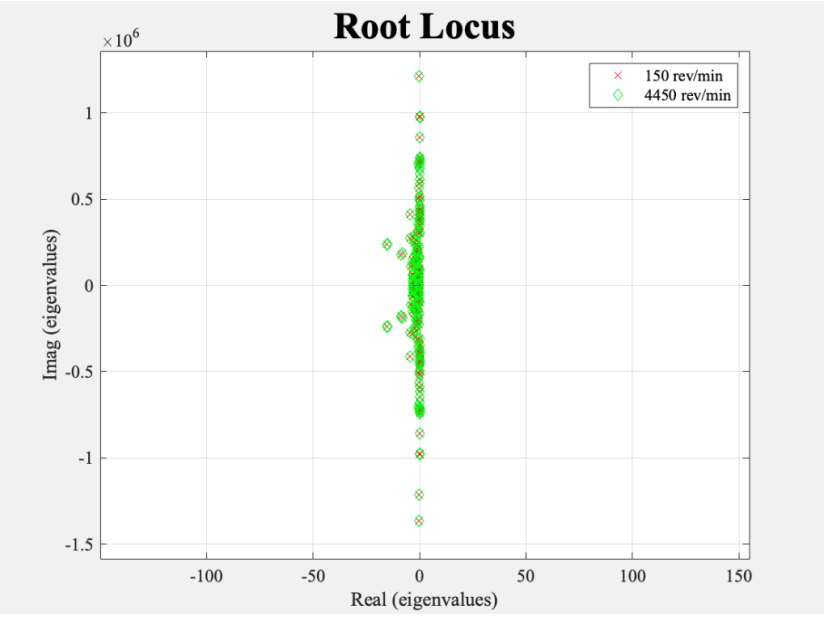

Figure 21:Root Locus for 150-4450 rpm

When we look at Figure 21, we can say that our system is stable since the real parts of all roots are negative or close to zero for 150 and 4450 rpm values.

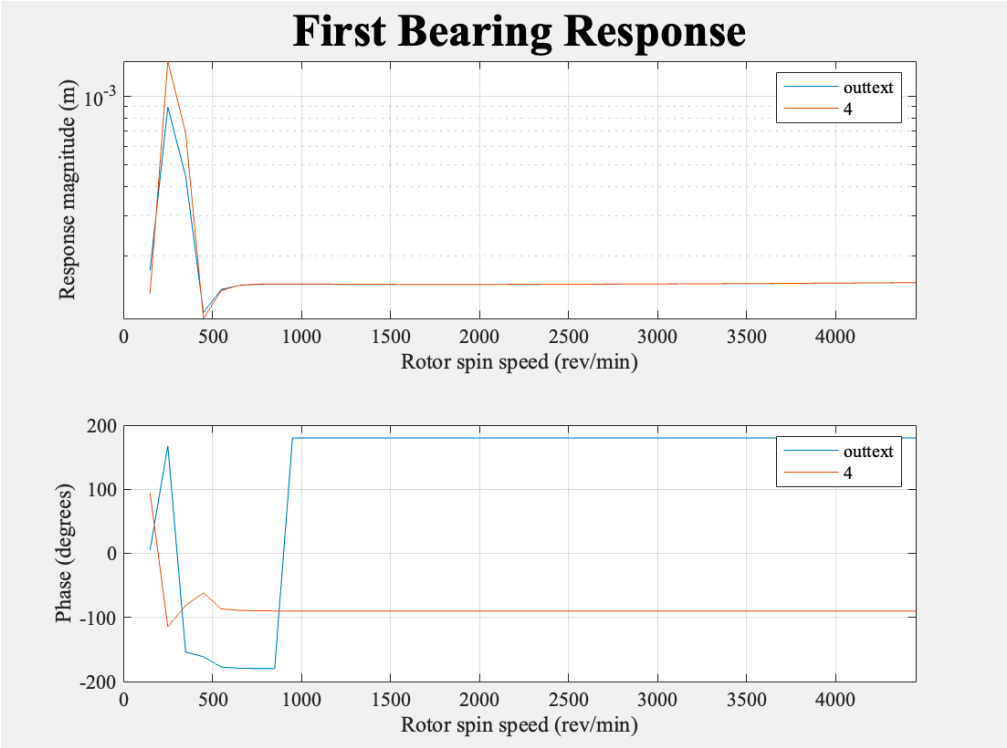

Figure 22:First Bearing Response (at Node 8)

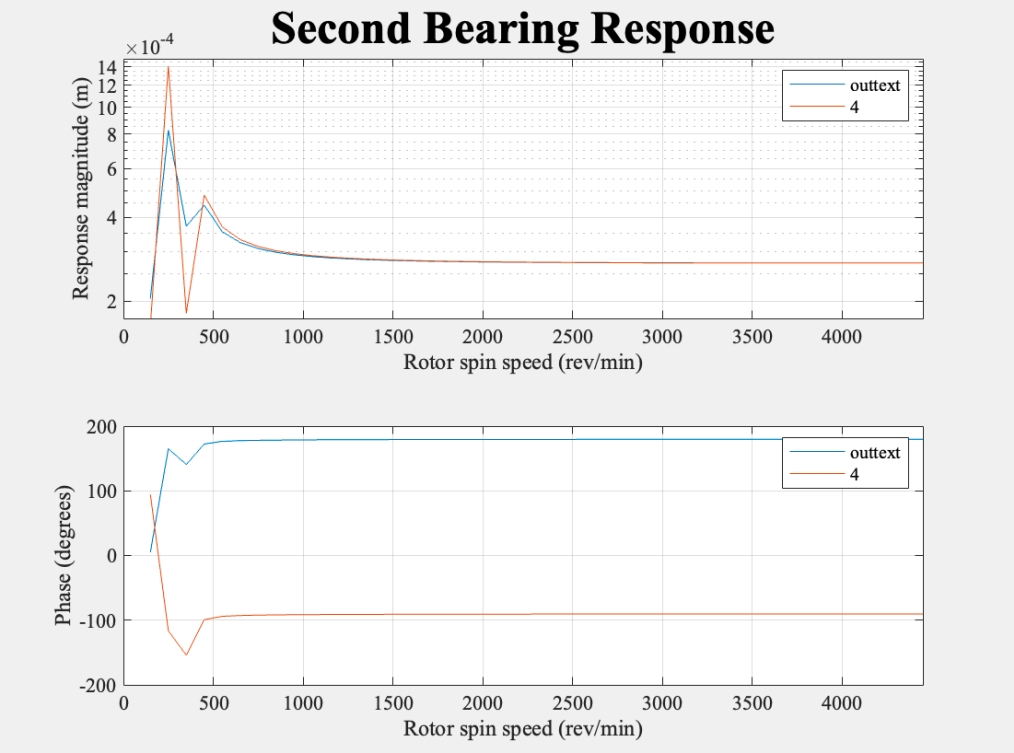

Figure 23: Second Bearing Response (at Node 37)

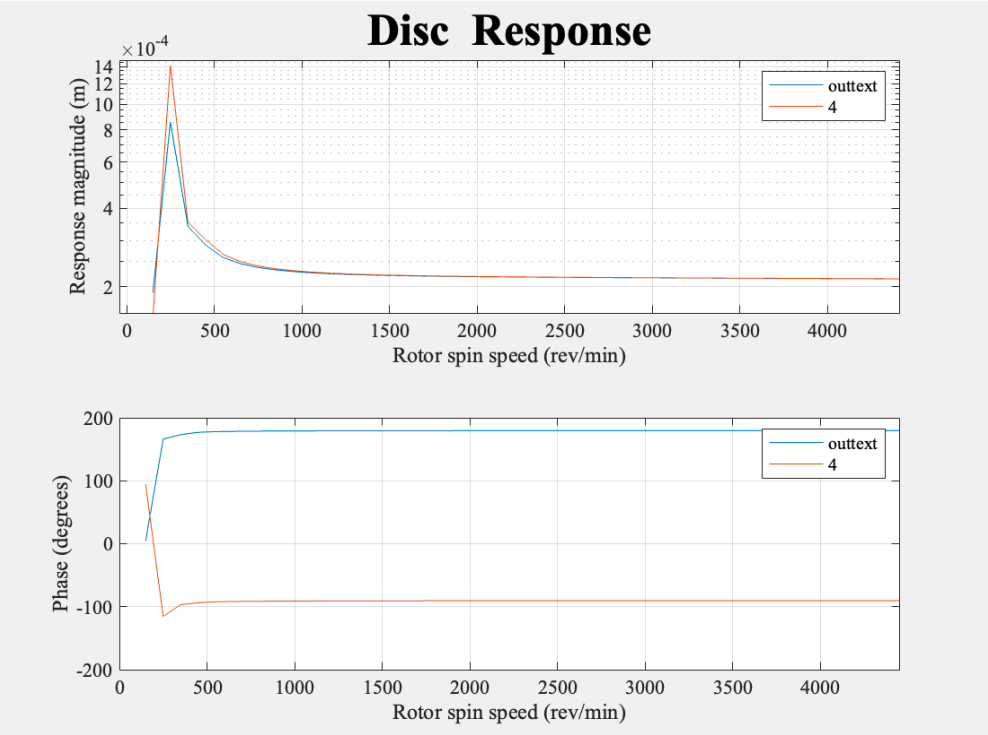

Figure 24:Disc Response (at node 19) Response for x and y directions

Looking at the First Bearing, Second Bearing and Disc Response graphs shown in Figures 22, 23 and 24, it is seen that the rotor resonates at almost the same frequency values in both x and y directions. At the rotation frequency where the rotor resonates, the response values increase dramatically.

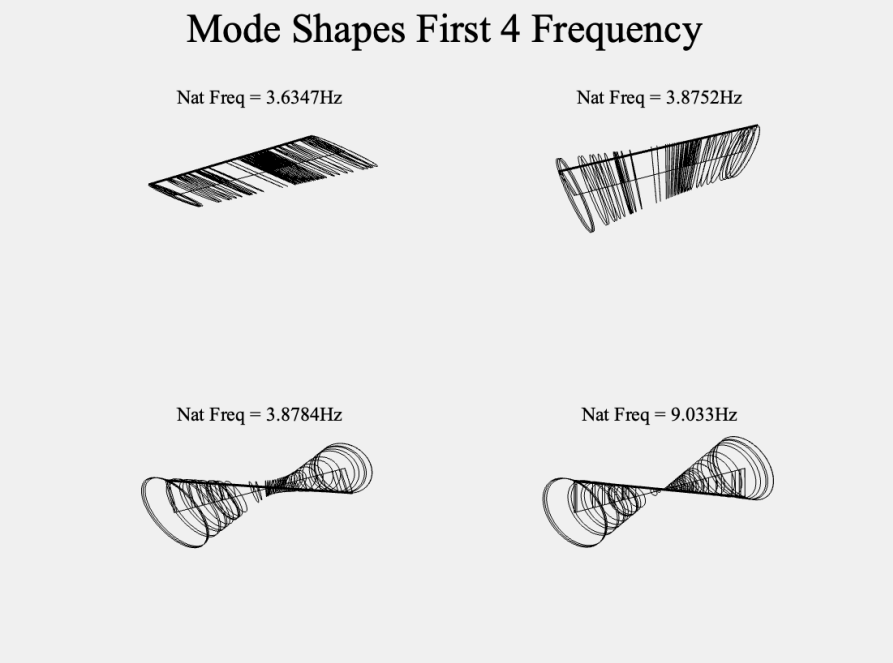

Figure 25:Mode Shapes for First 4 Frequency

Looking at Figure 25, the mode shapes of the first four natural frequency values of the shaft can be seen. This is important to observe how the displacement of the shaft changes at each node at these natural frequencies.

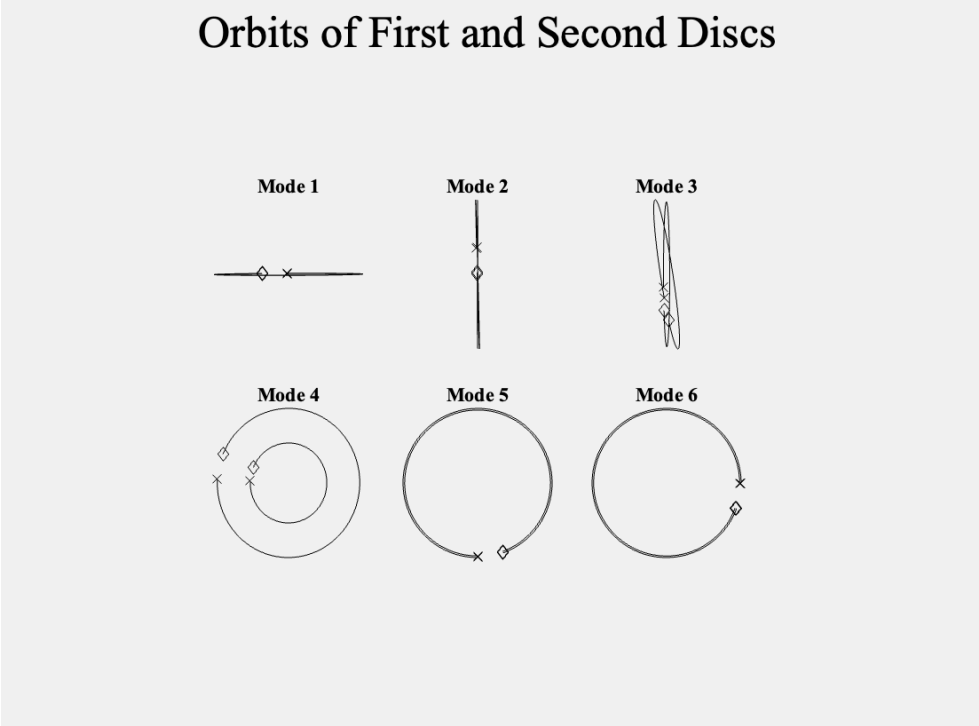

Figure 26:Orbits of First and Second Disks. The axial view of the mode shapes node 19 and node 21 for a rotor supported by constant stiffness and damping – diagonal, no rotational stiffness bearing at 3,000 rev/m in. The cross denotes the start of the orbit, and the diamond denotes the end.

For Figure 26, It is given using the kappa parameter based on the modal displacements in the two translational directions at each node of the FE model. If kappa is negative, the mode returns at that position; If kappa is positive, that mode rotates forward. The magnitude of K gives the aspect ratio of the ellipse. Mode 5 does backward whirl and modes 4 and 6 do forward whirl. However, there are mixed modes between modes 1 and 3, where the rotor rotates forward at some positions along the shaft and rotates backward at others. Figure 5.35 shows mode 5 and highlights that this mode rotates forward on the left disk (node 19) and rotates backward on the right disk (node 21). Only node 19 returns at mod 5, and the relative modal amplitude at this node is small.

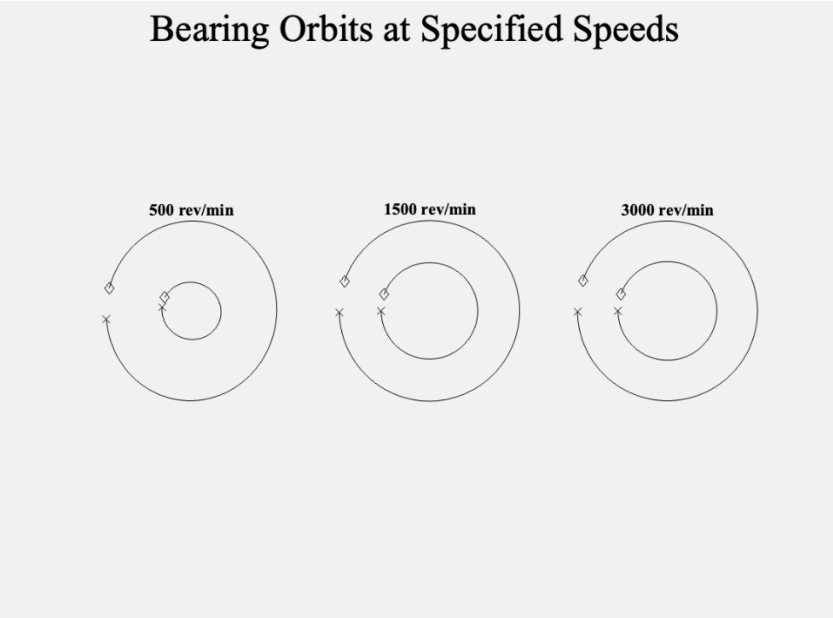

Figure 27: Orbits of First and Second Bearings The axial view of the mode shapes node 8 and node 37 for a rotor supported by constant stiffness and damping – diagonal, no rotational stiffness bearing at specified rotation speeds. The cross denotes the start of the orbit, and the diamond denotes the end.

According to Figure 27, specially selected values such as 500, 1500 and 3000 rpm indicate the Forward Whirl for both bearings located at nodes 8 and 37.

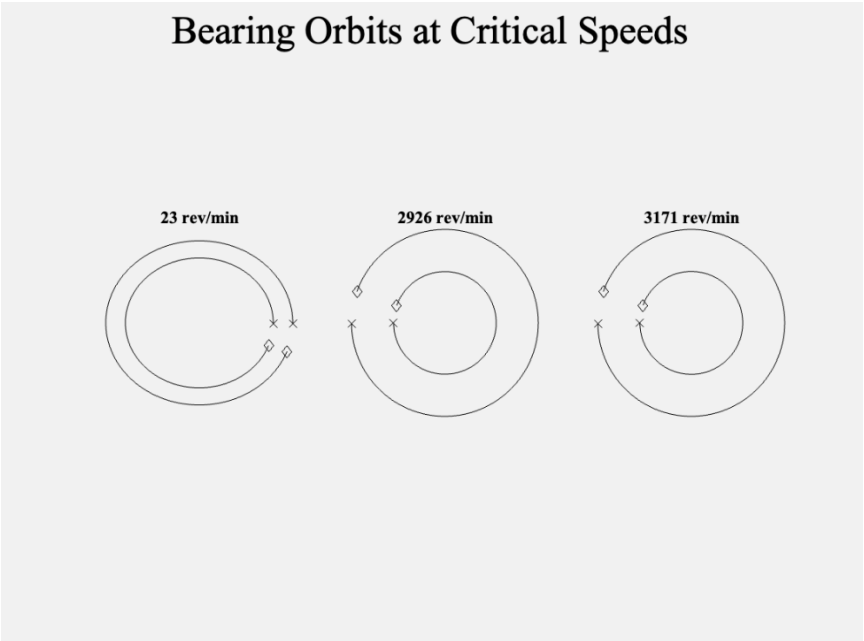

Figure 28: Orbits of First and Second Bearings The axial view of the mode shapes node 8 and node 37 for a rotor supported by constant stiffness and damping – diagonal, no rotational stiffness bearing at critical rotation speeds. The cross denotes the start of the orbit, and the diamond denotes the end.

When Figure 28 is examined, the vortex directions observed in the beds for three critical rotation speeds are shown. In all three cases there is Forward Whirling.

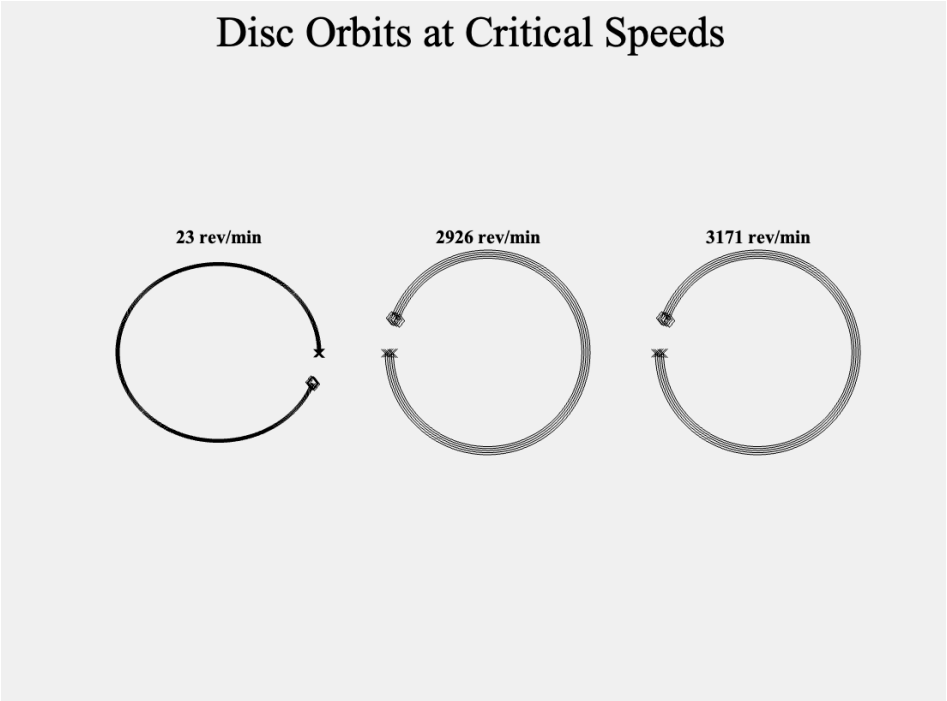

Figure 29: Orbits of First and Second Disc The axial view of the mode shapes node 19 and node 21 for a rotor supported by constant stiffness and damping – diagonal, no rotational stiffness bearing at critical rotation speeds. The cross denotes the start of the orbit, and the diamond denotes the end.

Examining Figure 29 shows the vorticity directions observed at nodes 19 and 21 in the disk for three critical rotation speeds. In all three cases there is Forward whirling.

Hydraulic bearings are often used in steam turbines because these bearings have the ability to operate at high speeds and can withstand high temperatures. In terms of damping, hydraulic bearings can absorb vibrations and reduce vibrations in the system, which can improve the stability of the turbine. Additionally, because hydraulic bearings generally have lower vibration levels, they can better control critical speeds, ensuring safe operation of the turbine. For these reasons, hydraulic bearings are often preferred in steam turbines.

```
Hydrodynamic brg, force = 1:1
Damped frequency at 3000rpm = 3.6326408400 Hz,  Zeta = 3.8725692037, kappa = 3.8741772788
Damped frequency at 3000rpm = 9.0221530913 Hz,  Zeta = 0.0332784006, kappa = 0.0365588324
Damped frequency at 3000rpm = 0.0468984490 Hz,  Zeta = 0.0490931995, kappa = -0.0145641729
Damped frequency at 3000rpm = -0.0045708115 Hz,  Zeta = -0.0822677891, kappa = 0.9551522681
Damped frequency at 3000rpm = -0.9978018398 Hz,  Zeta = 0.9979334447, kappa = -0.9996124728

Rotor speed = 3000 rev/min: ---
Somerfeld number = 0.71554
Eccentricity = 0.48436
Radial force = 536.8025N
Tangential force = 761.5081N
Gamma = 54.8192degrees

Crtical Speeds of Rotor
Critical Speeds; 23
Critical Speeds; 24
Critical Speeds; 35
Critical Speeds; 40
Critical Speeds; 2924
Critical Speeds; 3169
Critical Speeds; 4331
Critical Speeds; 5464
Critical Speeds; 7668
Critical Speeds; 10666
```

Figure 30: Script Result

7. COST ANALYSIS

The cost of a steam turbine rotor can vary considerably depending on the basic requirements and challenges faced by the industry needs and realities. The cost of designed for a rotor with a length of 1.2622 meters is as follows

- Materials cost, SAE 4140 (1.3mx0.2m nearly 1275 kg): $3500 - $5000
- Construction cost: $40,000 - $60,000
- Testing and quality: $10,000 - $15,000
- Shipping and handling: $ 5,000 - $ 10,000

  Combining these calculations, we can calculate the total cost of a steam turbine rotor with a period of 1.2622 m as follows.

Total cost = $58,500 to $135,000

Typically, a steam turbine rotor with a total length of 1.2622 meters costs between $58,500 and $135,000. These varieties are attributed to fabric choice, consistency, machinery, expensive warranties and prices. To obtain specific pricing it is important to negotiate with turbine manufacturers or suppliers who can offer different pricing based primarily on the specific characteristics and application requirements of the turbine.

8. CONCLUSION

In this study, we gained insight into how rotor dynamics simulations are performed. We observed that there were size differences in the response of the bearings. This difference is due to the bearings having different stiffness and damping values. Campbell diagrams were used to analyze critical velocities and resonance conditions. We learned that these diagrams help determine which modes are active and their characteristics when the rotor is operating at various speeds.

From the Root Locus graph, we conclude that the system is stable if the real part of the eigenvalues of the system lies on the left side of the graph. Regarding mode shapes, we found that as the natural frequency increases, the size and complexity of the conical modes also increase. This shows that the rotor will exhibit more pronounced and intense conical vibrations at higher frequencies. Specifically, we found that the conical shape in the mode shapes becomes more important as the natural frequency increases.

When comparing the orbits of the two selected disks, we found that some modes are of mixed type and that some of the remaining modes exhibit forward spin and some exhibit retrograde spin. This detailed understanding of the modes, shapes and dynamic behavior of the rotor is crucial for the design and analysis of rotor systems in practical applications.

References

[1] Krish Ramesh, Ph.D., Senior Product Technology Engineer, Introduction to Rotor Dynamics: A Physical Interpretation of the Principles and Application of Rotor Dynamics, Dresser-Rand, Houston, TX – 77043.

[2] Frisswell, M.I., Penny, J.E.T, Garvey, S.D., Lees, A.W.,(2010). Dynamics of Rotating Machines, 1st Edition., Cambridge University Press, New York, USA.

[3] Özdemir Mustafa, Prof, Mechanical Vibrations Lecture notes.

[4] Richard G. Budynas, J. Keith Nisbett , Shigley's Mechanical Engineering Design,9th Edition, McGraw-Hill , New York, USA.

[5] John Vance, Fouad Zeidan, Brian Murphy, MACHINERY VIBRATION AND ROTORDYNAMICS, John Wiley & Sons, Inc., Hoboken, New Jersey

[6] Nagaraju Tenali and Srinivas Kadivendi, ROTOR DYNAMIC ANALYSIS OF STEAM TURBINE ROTOR USING ANSYS , Int. J. Mech. Eng. & Rob. Res. 2014

[7] *https://www.hi-force.com/Admin/Content/Hydraulic-Oil-Health---Safety-Sheet54201623412.pdf*

Appendix A

Developed code for using Rotor Dynamics Software V2.

```
clear all;
clf;
clc;
set(0,'defaultaxesfontsize',12)
set(0,'defaultaxesfontname','Times New Roman')
set(0,'defaulttextfontsize',12)
set(0,'defaulttextfontname','Times New Roman')

% Rotor properties
E = 2.1e11;
nu = 0.25; %poisson ratio
rho = 7810;%density of rotor and blades
G=E/(2*(1+nu));%Shear modulus

%Diameters[m] ------------------------------------------------------------
-----------
ds = [0.075 0.071 0.063 0.136 0.063 0.110 0.100 0.100 0.100 ...
    0.125 0.125 0.125 0.125 0.125 0.245 0.362 0.180 0.1663 0.1408 0.1688...
    0.1433 0.1713 0.1453 0.1738 0.1483 0.1763 0.1508 0.1788 0.1533 0.1813
0.1558...
    0.1838 0.125 0.125 0.105 0.100 0.100 0.100 0.085 0.060 0.070 0.105
0.105]; % shaft diameter [m]
% element length [m]------------------------------------------------------
--------------%
le = [9 11 116.5 18 54 18 33.5 40 54.5 6 2 12.5 28 52.5 133.5 36 53.8...
    12.65 12.5 16.29 12.5 16.65 12.5 17.01 12.5 17.36 12.5 17.72 12.5...
    18.08 12.5 19.14 53 1 39 54.5 40 77 25 29.5 10 31 1]./1000;
% Disk diameter [m]
dd  = [215.02 216.94 220.19 223.36 226.51 229.88 233.13 236.5]./1000;
%disk Ip and Id calculation----------------------------------------------
--

disc_mass=[1.8147 1.8254 1.8714 1.9142 1.9589 2.0073 2.0554 2.1049];%[kg]
diao=[215.02 216.94 220.19 223.36 226.51 229.88 233.13 236.5]./1000;%[m]
diai=[ds(19) ds(21) ds(23) ds(25) ds(27) ds(29) ds(39) ds(43)];%[m]

A=pi./4.*(diao.^2-diai.^2);%Area of Disk
dh=disc_mass./(rho.*A);% Disk Thick

Ip=(disc_mass.*(diao.^2+diai.^2))./8;
Id=(0.5.*Ip)+(1/12.*disc_mass.*dh.^2);

% Hydrodynamic bearing properties
bl = 0.040; % length
bd = 0.100; % Diameter
rc = ds(8).*(0.15/100); % radial clearence %providing a clearance space
between the bush and the journal, which is typically between 0.1 and 0.2
percent of the journal diameter.
eta = 0.030; % dynamic oil viscosity from Reference [7]

% Timo 43 elements ------------------------------------------------
% Consider a model with elementh length
model.node = zeros((length(le)+1), 2);
model.node(:, 1) = 1:(length(le)+1);
```

```
cumulative_sum = 0; % starting value
for i = 1:(length(le)+1)
    model.node(i, 2) = cumulative_sum;
    if i <= (length(le))
        cumulative_sum = cumulative_sum + le(i);
    end
end


% Solid shaft
model.shaft = zeros(length(ds), 9);
model.shaft(:, 1) = 2;  % timoshenko
model.shaft(:, 4) = 0;  % outer dia
model.shaft(:, 5) = 0;% inner dia
model.shaft(:, 6) = rho; % Density
model.shaft(:, 7) = E;% Elastic modulus
model.shaft(:, 8) = G;% Shear modulus
model.shaft(:, 9) = 0;% There is no Damping in the shaft
% entering node in the matrix
for i = 1:length(ds)
    model.shaft(i, 2) = i;
    model.shaft(i, 3) = i + 1;
end

% ds valeu entering.
for i = 1:length(ds)
    model.shaft(i, 4) = ds(i);
end

%Defining Discs type and location
model.disc =   [2 19 disc_mass(1) Id(1) Ip(1);
                2 21 disc_mass(2) Id(2) Ip(2);
                2 23 disc_mass(3) Id(3) Ip(3);
                2 25 disc_mass(4) Id(4) Ip(4);
                2 27 disc_mass(5) Id(5) Ip(5);
                2 29 disc_mass(6) Id(6) Ip(6);
                2 39 disc_mass(7) Id(7) Ip(7);
                2 43 disc_mass(8) Id(8) Ip(8)];

%Calculating Shaft mass
shaft_mass=zeros(1,length(le));
for i=1:length(le)
    shaft_mass(i) = rho*le(i)*pi*(ds(i)^2)/4;
end
shaft_mass=sum(shaft_mass); % in kg

% disk_mass = rho*8*dh*pi*(dd^2-ds^2)/4;
disc_mass=sum(disc_mass);
brg_force = (shaft_mass+disc_mass)*9.81;%[N]
disp('Hydrodynamic brg, force = 1:1')


model.bearing = [3  8 49833 56618 144.05 160.14;
                 3 37 49326 56043 144.05 160.14];

% define the unbalance force at node 19 and 21
model.force = [1 19 0.03 0.0;
               1 21 0.01 0.0];
```

```
% Draw the rotor
figure(1), clf
picrotor(model)
title('Model of Rotor','FontSize',25);

% Plot the Campbell diagram and root locus
% ========================
% Define the rotor spin speed range
Rotor_Spd_rpm = 150:100:4500.0;
Rotor_Spd = 2*pi*Rotor_Spd_rpm/60; % convert to rad/s

% Calculate the eigensystem for the range of rotor spin speeds
[eigenvalues,eigenvectors,kappa,eccentricity] = chr_root(model,Rotor_Spd);

% Plot Campbell diagram
figure(2)
NX1 = 1;
damped_NF = 1; % plot damped natural frequencies
plotcamp(Rotor_Spd,eigenvalues,NX1,damped_NF,kappa)
title('Campbell Diagram ω_d','FontSize',25);

% plot undamped natural frequencies
figure(3);
plotcamp(Rotor_Spd,eigenvalues,1,0,kappa)
title('Campbell Diagram ω_n','FontSize',25);

%Root locus finding
NX2=2;
figure(4)
plotloci(Rotor_Spd,eigenvalues,NX2)
title('Root Locus','FontSize',25);

% plot the unbalance response
[response] = freq_rsp(model,Rotor_Spd);

figure(5) % Bearing responses at x axis
outnode = [8.1; 8.2];
plotresp(Rotor_Spd,response,outnode)
subplot(2,1,1);
title('First Bearing Response','FontSize',25)

figure(6) % Right Bearing Response
outnode = [37.1; 37.2];
plotresp(Rotor_Spd,response,outnode)
subplot(2,1,1);
title('Second Bearing Response','FontSize',25)

figure(7)
outnode = [19.1 19.2];
plotresp(Rotor_Spd,response,outnode)
subplot(2,1,1);
title('Disc  Response','FontSize',25)

% calculate eigenvalues at specified speed at 3000 rpm
Rotor_Spd_rpm = 3000;
Rotor_Spd = 2*pi*Rotor_Spd_rpm/60;  % convert to rad/s

[eigenvalues,eigenvectors,kap] = chr_root(model,Rotor_Spd);
Root = eigenvalues(1:2:8);
Nat_Freq_Hz = abs(Root)./(2*pi);
```

```
Damped_Nat_Freq_Hz = abs(imag(Root))./(2*pi); % s=-zeta*wn+-wn*sqrt(1-
zeta^2), wd=wn*sqrt(1-zeta^2)
zeta = -real(Root)./abs(Root);
kappa = kap(81,1:2:14); %kappa is the direction and size of the whirl
orbits, for both translations and rotations, at each node.
fprintf('Damped frequency at 3000rpm = %7.10f Hz,  Zeta = %6.10f, kappa =
%7.10f\n',Damped_Nat_Freq_Hz,zeta,kappa);
disp('  ')
%%
%Finding Sommerfeld Number from text book
F   = 0.5*brg_force;   % static load (N)
D   = bd;   % bearing diameter (m)
L   = bl;   % bearing length (m)
c   = rc; % bearing radial clearance (m)
L_rot=sum(le);
pressure = F/(L*D);

H = (8*c^2*F/(D*Rotor_Spd*eta*L^3))^2;
Ss = D*Rotor_Spd*eta*L^3/(8*F*c^2);
S = (Ss/pi)*(D/L)^2; % Sommerfeld Number

n2all = sort(roots([1 -4 (6-(16-pi^2)/H) -(4+pi^2/H) 1]));
nroot = 0; n2 = []; % test roots - eccentricity should be between 0 and 1
for ir=1:4
    nn = n2all(ir);
    if nn>0 && nn<1 && isreal(nn)
        nroot = nroot + 1;
        n2 = [n2; nn];
    end
end
if nroot == 0
    n2 = 0.5;
    disp('Error in calculating fluid bearing coefficents - no solutions for
eccentricity')
end
if nroot >= 2
    n2 = min(n2);
    disp('Error in calculating fluid bearing coefficents - multiple
solutions for eccentricity')
end

% Compute Radial and Tangential Force Note:n is eccentricity in code.
a = zeros(2,2); b = zeros(2,2);
n = sqrt(n2); q1 = (1-n2); q2 = (1+n2); q3 = (1+2*n2); p2 = pi^2;

fr = D*Rotor_Spd*eta*L^3*n^2/(2*c^2*(1-n^2)^2);%radial force  equation 5.81
ft = pi*D*Rotor_Spd*eta*L^3*n/(8*c^2*(1-n^2)^1.5);%tan force
gamma = atan(ft/fr);
gamma_degree = gamma*180/pi;

disp(['Rotor speed = ' num2str(Rotor_Spd_rpm) ' rev/min: ---'])
disp(['Somerfeld number = ' num2str(S)]);
disp(['Eccentricity = ' num2str(n)]);
disp(['Radial force = ' num2str(fr) 'N']);
disp(['Tangential force = ' num2str(ft) 'N']);
disp(['Gamma = ' num2str(gamma_degree) 'degrees']);
disp('  ')
%-------------------------------------------------------------------------
```

```
% Plot the modes and orbits at 3000 rev/min %
=========================================
[eigenvalues,eigenvectors,kappa] = chr_root(model,Rotor_Spd);
figure(8)
subplot(221)
plotmode(model,eigenvectors(:,1),eigenvalues(1))
subplot(222)
plotmode(model,eigenvectors(:,3),eigenvalues(3))
subplot(223)
plotmode(model,eigenvectors(:,5),eigenvalues(5))
subplot(224)
plotmode(model,eigenvectors(:,7),eigenvalues(7))
sgtitle('Mode Shapes First 4 Frequency','FontSize',25)

% plot orbits first and second Disk
figure(9)
outputnode = [19; 21];
axes('position',[0.2 0.53 0.2 0.2 ])
plotorbit(eigenvectors(:,1),outputnode,'Mode 1',eigenvalues(1))
axes('position',[0.39 0.53 0.2 0.2 ])
plotorbit(eigenvectors(:,3),outputnode,'Mode 2',eigenvalues(3))
axes('position',[0.58 0.53 0.2 0.2 ])
plotorbit(eigenvectors(:,5),outputnode,'Mode 3',eigenvalues(5))
axes('position',[0.2 0.25 0.2 0.2 ])
plotorbit(eigenvectors(:,7),outputnode,'Mode 4',eigenvalues(7))
axes('position',[0.39 0.25 0.2 0.2 ])
plotorbit(eigenvectors(:,9),outputnode,'Mode 5',eigenvalues(9))
axes('position',[0.58 0.25 0.2 0.2 ])
plotorbit(eigenvectors(:,11),outputnode,'Mode 6',eigenvalues(11))
sgtitle('Orbits of First and Second Discs','FontSize',25)

% Bearing Orbits
Rotor_Spd_rpm = [500 1500 3000];
Rotor_Spd = 2*pi*Rotor_Spd_rpm/60;  % convert to rad/s
[response] = freq_rsp(model,Rotor_Spd);

figure(10), clf
outputnode = [8 37];
subplot(131)
plotorbit(response(:,1),outputnode,'500 rev/min')
subplot(132)
plotorbit(response(:,2),outputnode,'1500 rev/min')
subplot(133)
plotorbit(response(:,3),outputnode,'3000 rev/min')
sgtitle('Bearing Orbits at Specified Speeds','FontSize',25)

%Critical Speeds Bearing orbits
Rotor_Spd_rpm = [23 2926 3171];
Rotor_Spd = 2*pi*Rotor_Spd_rpm/60;  % convert to rad/s
[response] = freq_rsp(model,Rotor_Spd);
figure(11), clf
outputnode = [8 37];
subplot(131)
plotorbit(response(:,1),outputnode,'23 rev/min')
subplot(132)
plotorbit(response(:,2),outputnode,'2926 rev/min')
subplot(133)
plotorbit(response(:,3),outputnode,'3171 rev/min')
sgtitle('Bearing Orbits at Critical Speeds','FontSize',25)
%Critical Speeds Disks
```

```
Rotor_Spd_rpm = [23 2926 3171];
Rotor_Spd = 2*pi*Rotor_Spd_rpm/60;  % convert to rad/s
[response] = freq_rsp(model,Rotor_Spd);

figure(12), clf
outputnode = [19 21 23 25 27];
subplot(131)
plotorbit(response(:,1),outputnode,'23 rev/min')
subplot(132)
plotorbit(response(:,2),outputnode,'2926 rev/min')
subplot(133)
plotorbit(response(:,3),outputnode,'3171 rev/min')
sgtitle('Disc Orbits at Critical Speeds','FontSize',25)

Rotor_Spd_rpm = 150:100:11500.0;
Rotor_Spd = 2*pi*Rotor_Spd_rpm/60;  % convert to rad/s
[eigenvalues,eigenvectors,kappa] = chr_root(model,Rotor_Spd);

[critical_speeds2,mode_shape2] = crit_spd(model,1,0,10);

disp('Crtical Speeds of Rotor ')
fprintf('Critical Speeds; %.f\n',critical_speeds2)
```

Appendix B

Referance source tables.

Table 1: Sectional Proprieties			
Section No.	Length(L) (mm)	Diameter(D) (mm)	Temp °
1	09.00	75	60
2	11.00	71	60
3	116.50	63	60
4	18.00	136	60
5	54.00	63	60
6	18.00	110	60
7	33.50	100	60
8	40.00	100	60
9	54.50	100	60
13	06.00	125	197
14	02.00	125	207
15	12.5	125	250
16	28	125	260
17	52.5	125	280
18	133.5	245	480
19	36	362	486
20	53.8	180	313
21	12.65	166.3	455
22	12.5	140.8	449
23	16.29	168.8	444
24	12.5	143.3	438
25	16.65	171.3	432
26	12.5	145.3	438
27	17.01	173.8	419
28	12.5	148.3	412
29	17.36	176.3	405
30	12.5	150.8	398
31	17.72	178.8	390
32	12.50	153.3	382
33	18.08	181.3	373
34	12.50	155.8	364
35	19.14	183.8	354
39	53.00	125	200
40	1.00	125	106
41	39.00	105	60
42	54.50	100	60
43	40.00	100	60
44	77.00	100	60
45	25.00	85	60
46	29.50	60	60
47	10.00	70	60
48	31.00	105	60
49	1.00	105	60

Table 2: Desk Input Data			
Disk No.	Mass of Disk (kg)	Equivalent Diameter	Section Location
1	1.8147	215.02	22
2	1.8254	216.94	24
3	1.8714	220.19	26
4	1.9142	223.36	28
5	1.9589	226.51	30
6	2.0073	229.88	32
7	2.0554	233.13	45
8	2.1049	236.5	49

Table 3: Bearing Details				
	Length (mm)	Diameter (mm)	Section Location	Type of bearing
Front Bearing	40	100	8	Tilting pad
Rear Bearing	40	100	43	Tilting pad

Table 4: Properties for 1st Bearing								
Speed (RPM)	**$K_{XX}\times 10^3$**	**K_{XY}**	**K_{YX}**	**$K_{YY}\times 10^3$**	**$C_{XX}\times 10^3$**	**C_{XY}**	**C_{YX}**	**$C_{YY}\times 10^3$**
671.3	27003	0	0	29272	155.26	0	0	193.35
1342.6	32701	0	0	36101	152.46	0	0	185.05
2013.9	38414	0	0	42945	149.66	0	0	176.75
2685.3	44127	0	0	49789	146.86	0	0	168.44
3356.6	49833	0	0	56618	144.05	0	0	160.14
4292	57749	0	0	66146	140.11	0	0	148.52
4703.2	61289	0	0	70336	138.45	0	0	143.54
5361.3	66893	0	0	77090	135.75	0	0	135.34
5610.3	69023	0	0	79633	134.71	0	0	132.43
6411.7	75818	0	0	87804	131.39	0	0	122.57
7205.9	82545	0	0	95859	128.07	0	0	112.61
8014.7	89459	0	0	104093	124.65	0	0	102.75
8825.1	96395	0	0	112413	121.33	0	0	92.89
9637.3	103276	0	0	120663	118	0	0	82.92
10403.1	109674	0	0	128443	114.68	0	0	73.07
11000	115566	0	0	135608	111	0	0	63.12
12000	125388	0	0	147551	107	0	0	51.02
13000	135209	0	0	159494	102	0	0	38.25

Table 5: Properties for 2nd Bearing								
Speed (RPM)	**$K_{XX}\times 10^3$**	**K_{XY}**	**K_{YX}**	**$K_{YY}\times 10^3$**	**$C_{XX}\times 10^3$**	**C_{XY}**	**C_{YX}**	**$C_{YY}\times 10^3$**
664.5	26729	0	0	28975	155.26	0	0	193.35
1329	32369	0	0	35734	152.46	0	0	185.05
1993.5	38024	0	0	42509	149.66	0	0	176.75
2658	43679	0	0	49283	146.86	0	0	168.44
3322.5	49326	0	0	56043	144.05	0	0	160.14
4248.4	57163	0	0	65474	140.11	0	0	148.52
4655.4	60666	0	0	69622	138.45	0	0	143.54
5553.3	68322	0	0	78824	134.71	0	0	132.43
6346.6	75047	0	0	86911	131.39	0	0	122.57
7132.6	81706	0	0	94885	128.07	0	0	112.61
7933.2	88550	0	0	103035	124.65	0	0	102.75
8735.5	95415	0	0	111270	121.33	0	0	92.89
9539.3	102226	0	0	119436	118	0	0	82.92
10297.4	108559	0	0	127137	114.68	0	0	73.07
11000	114392	0	0	134230	111	0	0	63.12
12000	122724	0	0	144363	107	0	0	51.02
13000	131057	0	0	154495	102	0	0	38.25